Advanced Measurement Concepts for Mid-infrared Semiconductor Laser based Trace Gas Sensor Technologies: Opportunities & Challenges

Frank K. Tittel
Department of Electrical and Computer Engineering,
Rice University, Houston, TX 77005, USA
http://www.ece.rice.edu/~lasersci/

OUTLINE

- New Laser Based Trace Gas Sensor Technology
  - Novel Multipass Gas Absorption Cells & Electronics
  - Quartz Enhanced Photoacoustic Spectroscopy
- Examples of nine Mid-infrared Trace Gas Species
  - C_2H_6, NH_3, NO, CO, SO_2, CH_4, N_2O, H_2O_2 & C_3H_6O
- Future Directions of Laser Based Trace Gas Sensor Technologies and Conclusions

CPPTA
Warsaw, Poland

Sept. 23-26, 2014

Research support by NSF ERC MIRTHE, NSF-ANR NexCILAS, the Robert Welch Foundation, and Sentinel Photonics Inc. via an EPA Phase 1 SBIR sub-award is acknowledged

Wide Range of Trace Gas Sensing Applications

- **Urban and Industrial Emission Measurements**
  - Industrial Plants
  - Combustion Sources and Processes (e.g. fire detection)
  - Automobile, Truck, Aircraft and Marine Emissions
- **Rural Emission Measurements**
  - Agriculture & Forestry, Livestock
- **Environmental Monitoring**
  - Atmospheric Chemistry (e.g isotopologues, climate modeling,…)
  - Volcanic Emissions
- **Chemical Analysis and Industrial Process Control**
  - Petrochemical, Semiconductor, Pharmaceutical, Metals Processing, Food & Beverage Industries, Nuclear Technology & Safeguards
- **Spacecraft and Planetary Surface Monitoring**
  - Crew Health Maintenance & Life Support
- **Applications in Medical Diagnostics and the Life Sciences**
- **Technologies for Law Enforcement, Defense and Security**
- **Fundamental Science and Photochemistry**

RICE

“Curiosity” Landed on Mars on August 6, 2012

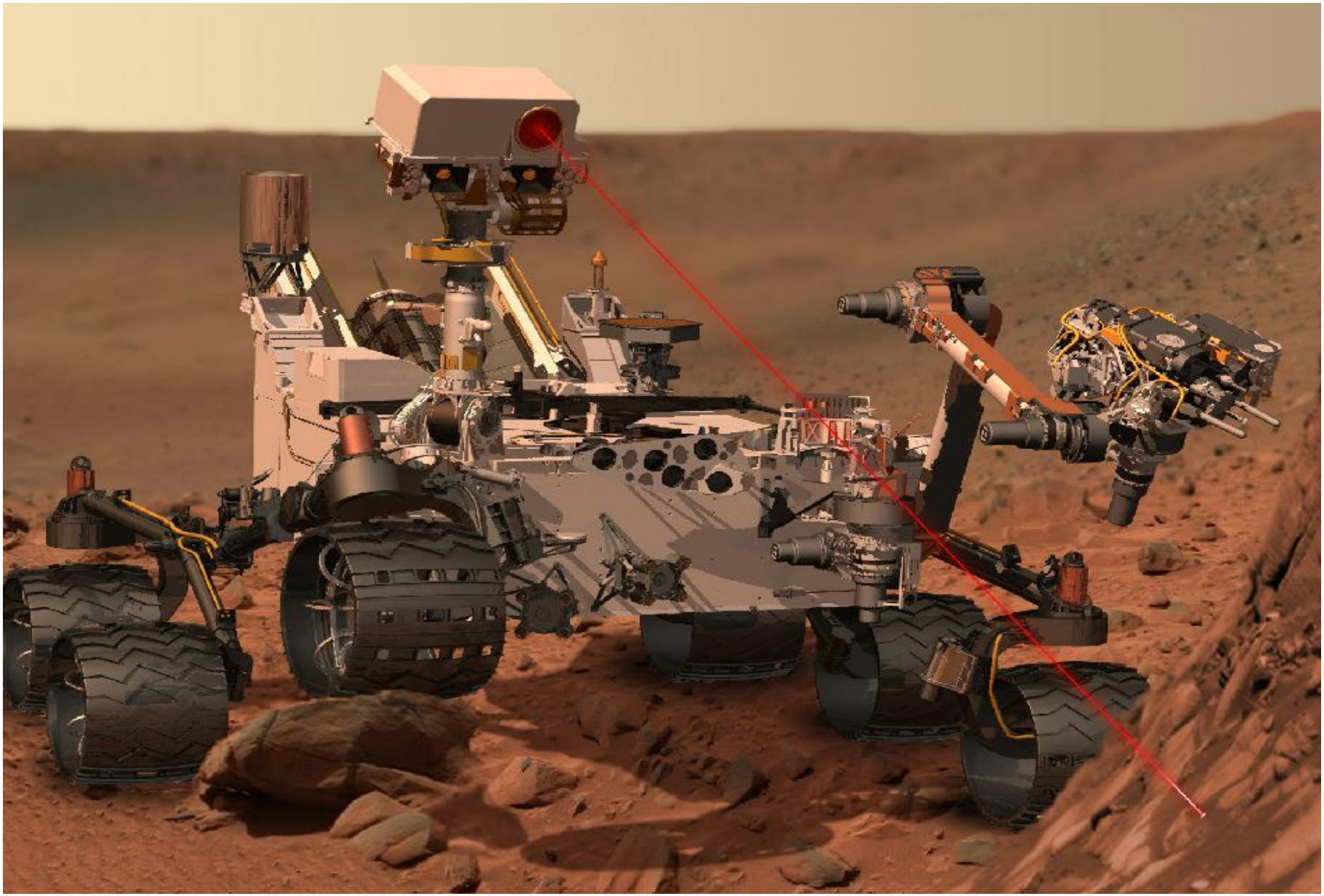

Laser based Trace Gas Sensing Techniques

- **Optimum Molecular Absorbing Transition**
  - Overtone or Combination Bands (NIR)
  - Fundamental Absorption Bands (Mid-IR)
- **Long Optical Pathlength**
  - Multipass Absorption Cell (White, Herriot, Chernin, Sentinel Photonics/Aeris Technologies)
  - Cavity Enhanced and Cavity Ringdown Spectroscopy
  - Open Path Monitoring (with retro-reflector): Standoff and Remote Detection
  - Fiberoptic Evanescent Wave Spectroscopy
- **Spectroscopic Detection Schemes**
  - Frequency or Wavelength Modulation
  - Balanced Detection
  - Zero-air Subtraction
  - Photoacoustic & Quartz Enhanced Photoacoustic Spectroscopy (QEPAS)

RICE

Demonstration of CH4 Sensor Performance

- Develop of Protoype Package in Year 1
- Develop of 2nd Generation Sensor System Year 2
- Develop Pre-Production Package

RICE

HITRAN Simulated Mid-Infrared Molecular Absorption Spectra

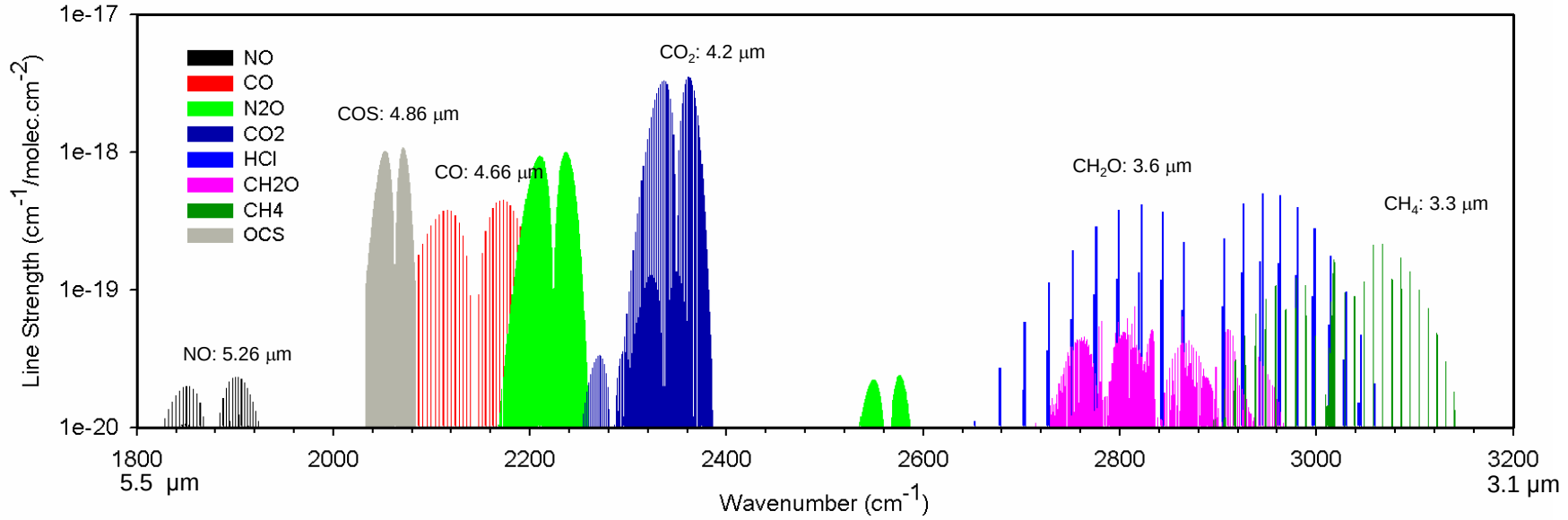

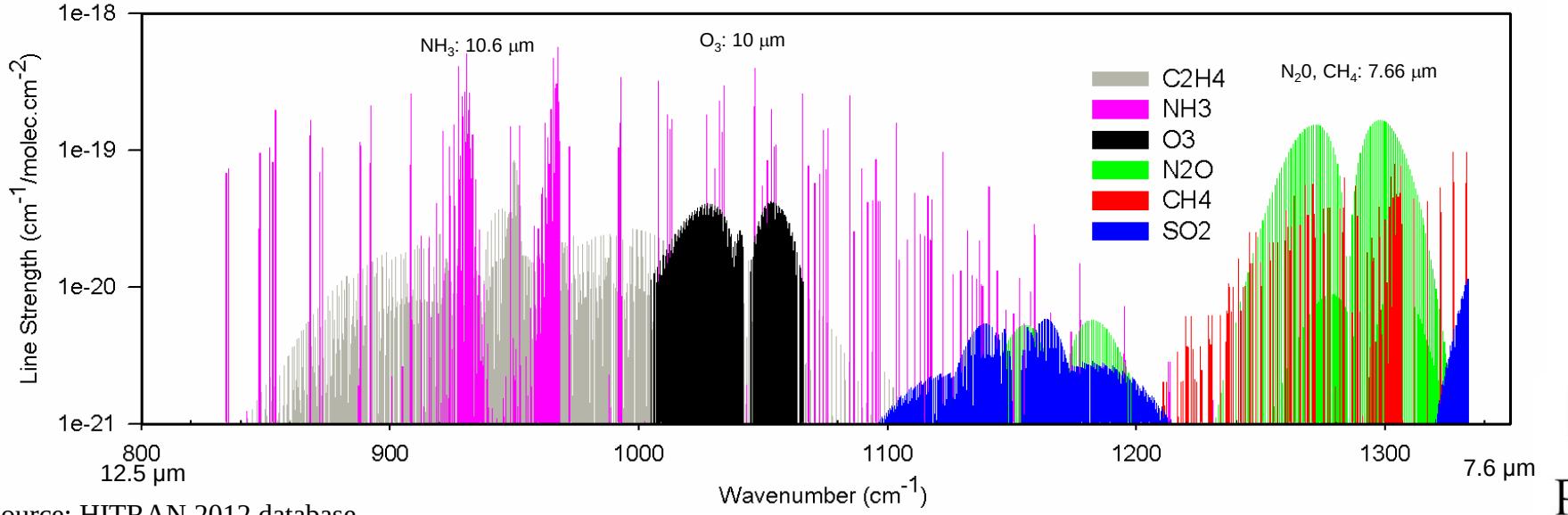

Source: HITRAN 2012 database

RICE

Mid-IR Source Requirements for Laser Spectroscopy

REQUIREMENTS	IR LASER SOURCE
Sensitivity (% to pptv)	Optimum Wavelength, Power
Selectivity (Spectral Resolution)	Stable Single Mode Operation and Narrow Linewidth
Multi-gas Components, Multiple Absorption Lines and Broadband Absorbers	Mode Hop-free Wavelength Tunability
Directionality or Cavity Mode Matching	Beam Quality
Rapid Data Acquisition	Fast Time Response
Room Temperature Operation	High wall plug efficiency, no cryogenics or cooling water
Field deployable in harsh environments	Compact & Robust

Key Characteristics of Mid-IR QCL & ICL Sources – Sept. 2014

- **Band – structure engineered devices**
  Emission wavelength is determined by layer thickness – MBE or MOCVD; Type I QCLs operate in the 3 to 24 μm spectral region; Type II and GaSb based ICLs can cover the 3 to 6 μm spectral range.
  - Compact, reliable, stable, long lifetime, and commercial availability
  - Fabry-Perot (FP), single mode (DFB) and multi-wavelength devices

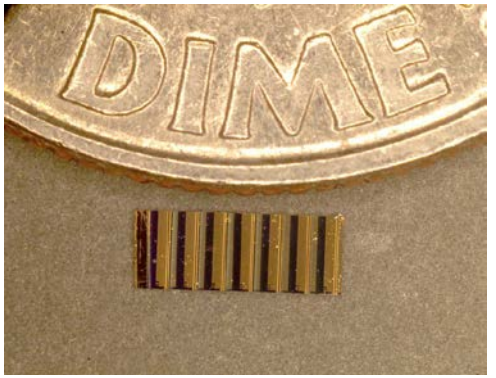

4 mm

- **Wide spectral tuning ranges in the mid-IR**
  - 1.5 cm^{-1} using injection current control for DFB devices
  - 10-20 cm^{-1} using temperature control for DFB devices
  - ~100 cm-1 using current and temperature control for QCL DFB Array
  - ~ 525 cm^{-1} (22% of c.w.) using an external grating element and FP chips with heterogeneous cascade active region design; also QCL DFB Array

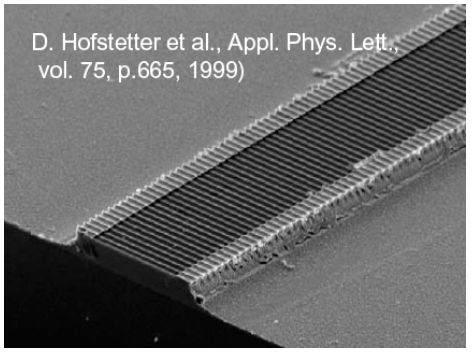

- **Narrow spectral linewidths**
  - CW: 0.1 - 3 MHz & <10kHz with frequency stabilization (0.0004 cm^{-1})
  - Pulsed: ~ 300 MHz

- **High pulsed and CW powers of QCLs at TEC/RT temperatures**
  - Room temperature pulsed power of > 30 W with 44% wall plug efficiency
  - CW powers of ~ 5 W with 23% wall plug efficiency at 293 ºK
  - > 600 mW CW DFB @ 285 ºK; wall plug efficiency 23% at 4.6 μm

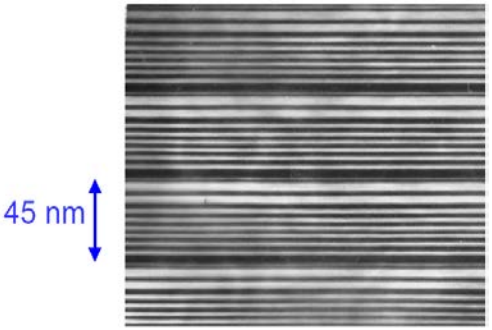

Motivation for Mid-infrared C_2H_6 Detection

- **Applications in medical breath analysis**
  - Asthma
  - Schizophrenia
  - Lung cancer
  - Vitamin E deficiency
- **Applications in atmospheric chemistry and climate R &D**
  - Fossil fuel and biofuel consumption
  - Biomass burning
  - Vegetation/soil
  - Natural gas loss

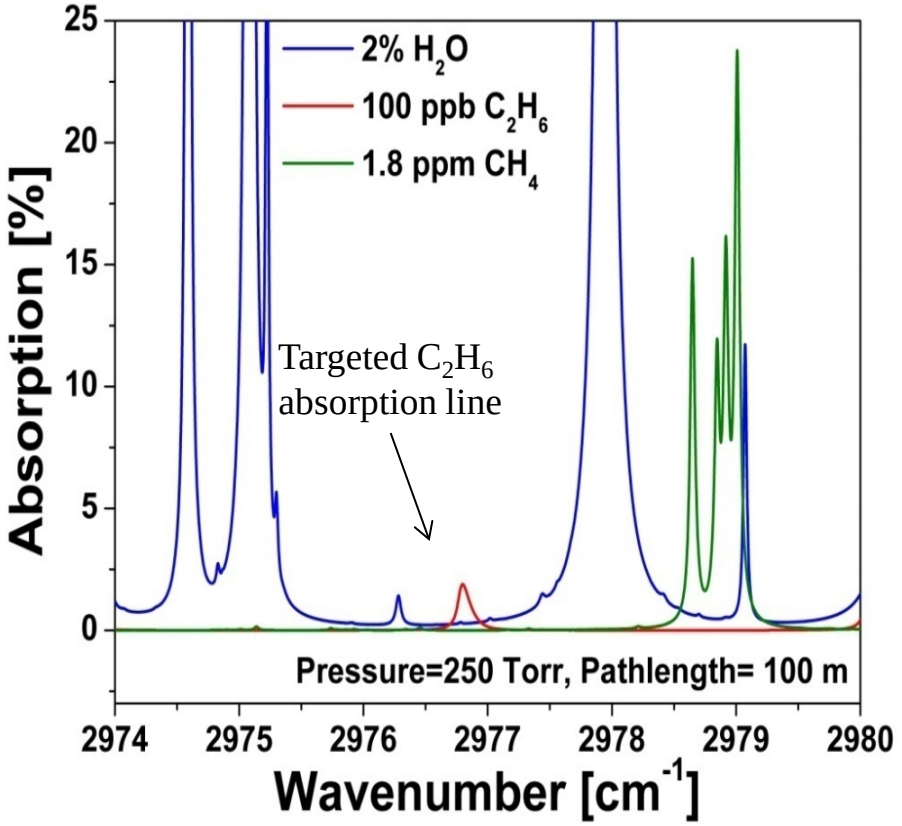

HITRAN absorption spectra of C_2H_6, CH_4, and H_2O

K. Krzempek et. al., Appl. Phys. B, 112, 461-465, 2013

RICE

C_2H_6 Detection with a 3.36 µm CW DFB LD using a Novel Compact Multipass Absorption Gas Cell and Control Electronics

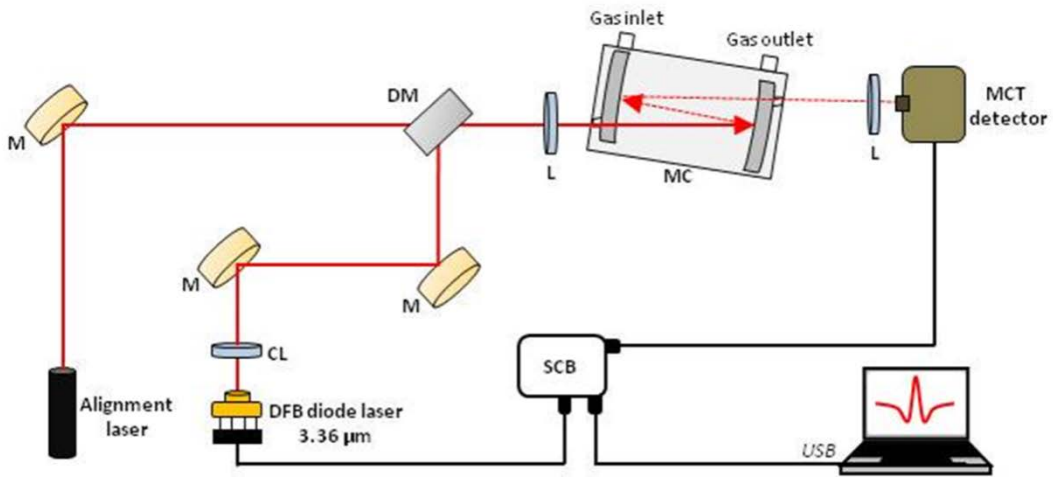

Schematic of a C_2H_6 gas sensor using a Nanoplus 3.36 µm DFB laser diode. M – mirror, CL – collimating lens, DM – dichroic mirror, MC – multipass cell, L – lens, SCB – sensor control board.

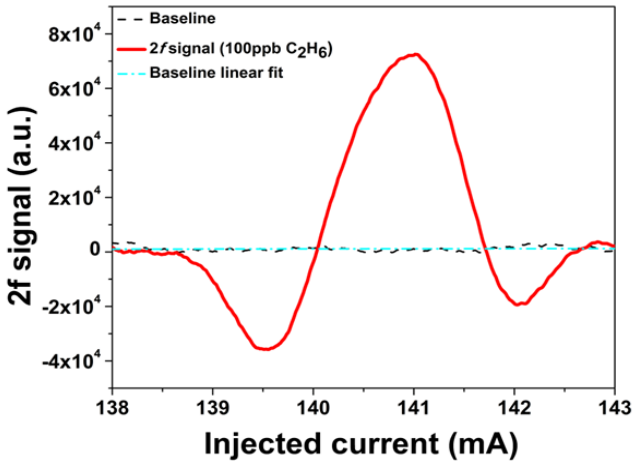

2f WMS signal for a C_2H_6 line at 2976.8 cm^{-1} at 200 Torr

Minimum detectable C_2H_6 concentration:
~ 740 pptv (1σ; 1 s time resolution)

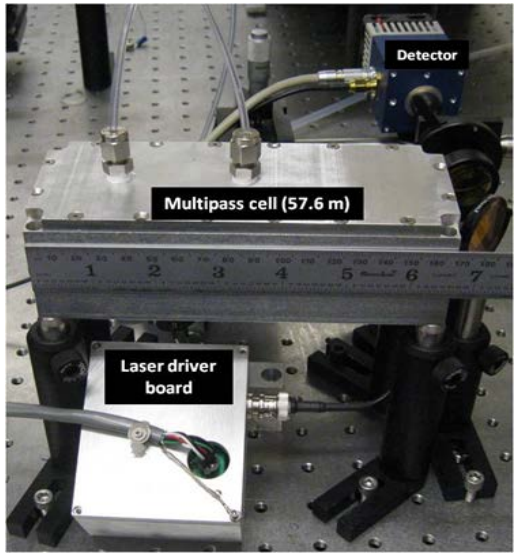

Innovative long path, small volume multipass gas cell: **57.6 m with 459 passes**

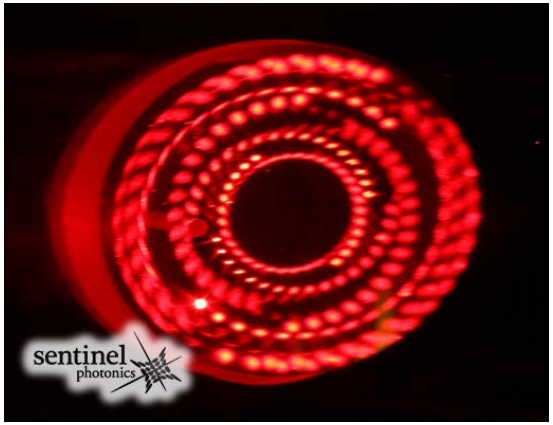

MGC dimensions: **17 x 6.5 x 5.5 (cm)**
Distance between the MGC mirrors: 12.5 cm

Typical Oil & Gas Production Site near Houston, TX

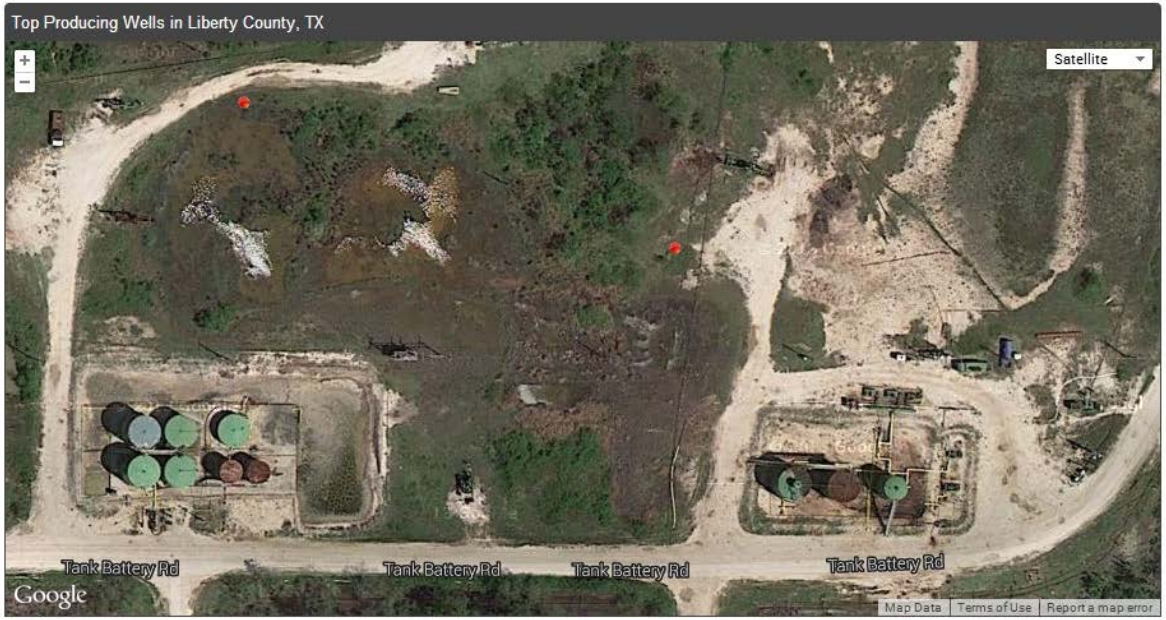

This figure shows the result of a sequence of four fracking injections obtained by directional drilling, which creates horizontal production in target stratum.

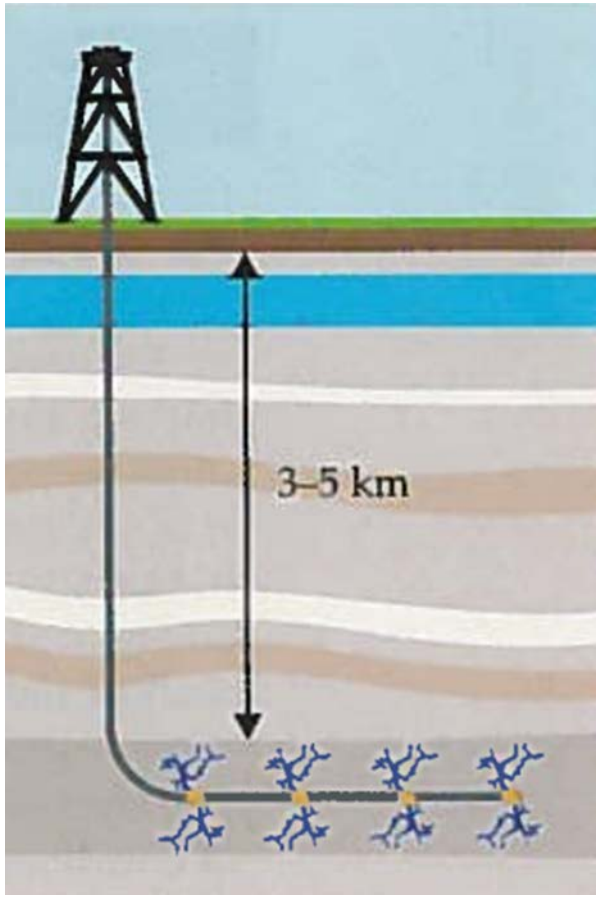

A proposed DOE-ARPA-E CH4 detection project at 3.327 μm will start in 2015 at a well platform of 10 m x10 m with a 1 m spatial resolution.

RICE

Oil in Water Detection

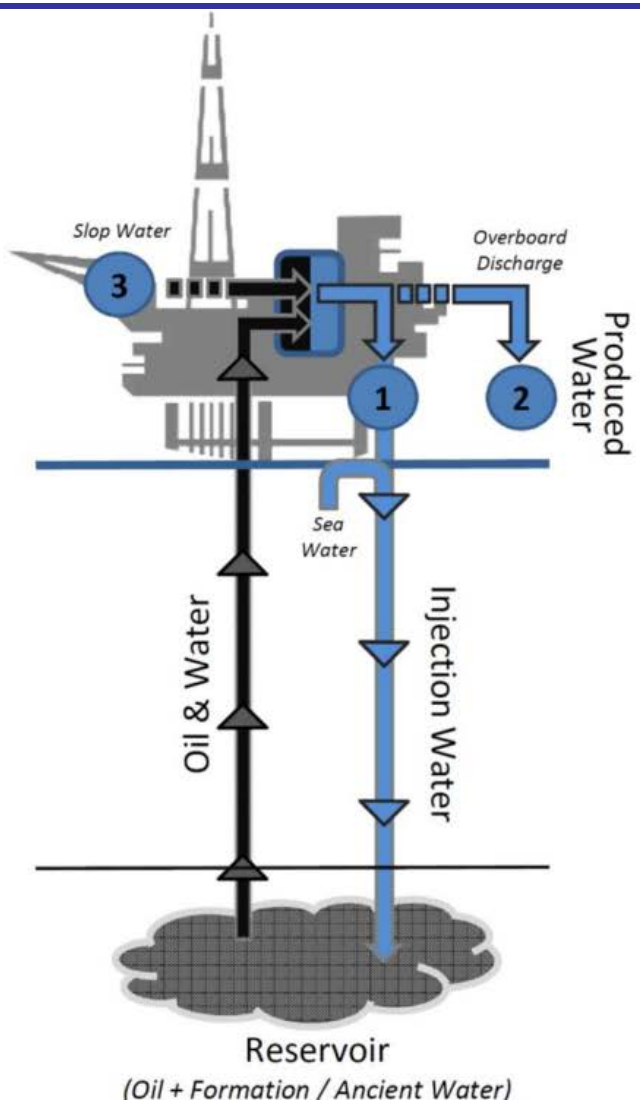

- Produced water
  - legislation: < 15 ppm
- Injection water
  - Economic reasons
    target value: < 5 ppm or lower

IQCLSW 2014, Policore, Italy: B. Lendl et al, Vienna University of Technology, Austria

Motivation for NH_3 Detection

- **Medical diagnostics**
  - Kidney disease
  - Liver failure and Cirrhosis
  - Brain Cells dysfunction
  - Drowsiness and Coma
- **Atmospheric chemistry**
- **Pollutant gases monitoring**
- **Monitoring NH_3 concentrations in the exhaust stream of NO_x removal systems based on selective catalytic reduction (SCR) techniques associated with electric power plants**
- **Spacecraft related trace gas monitoring**

RICE

Conventional Photoacoustic Spectroscopy (PAS)

Cell is OPTIONAL!

***V*-effective volume**

Laser beam, power P

Modulated (P or λ) at f or $f/2$

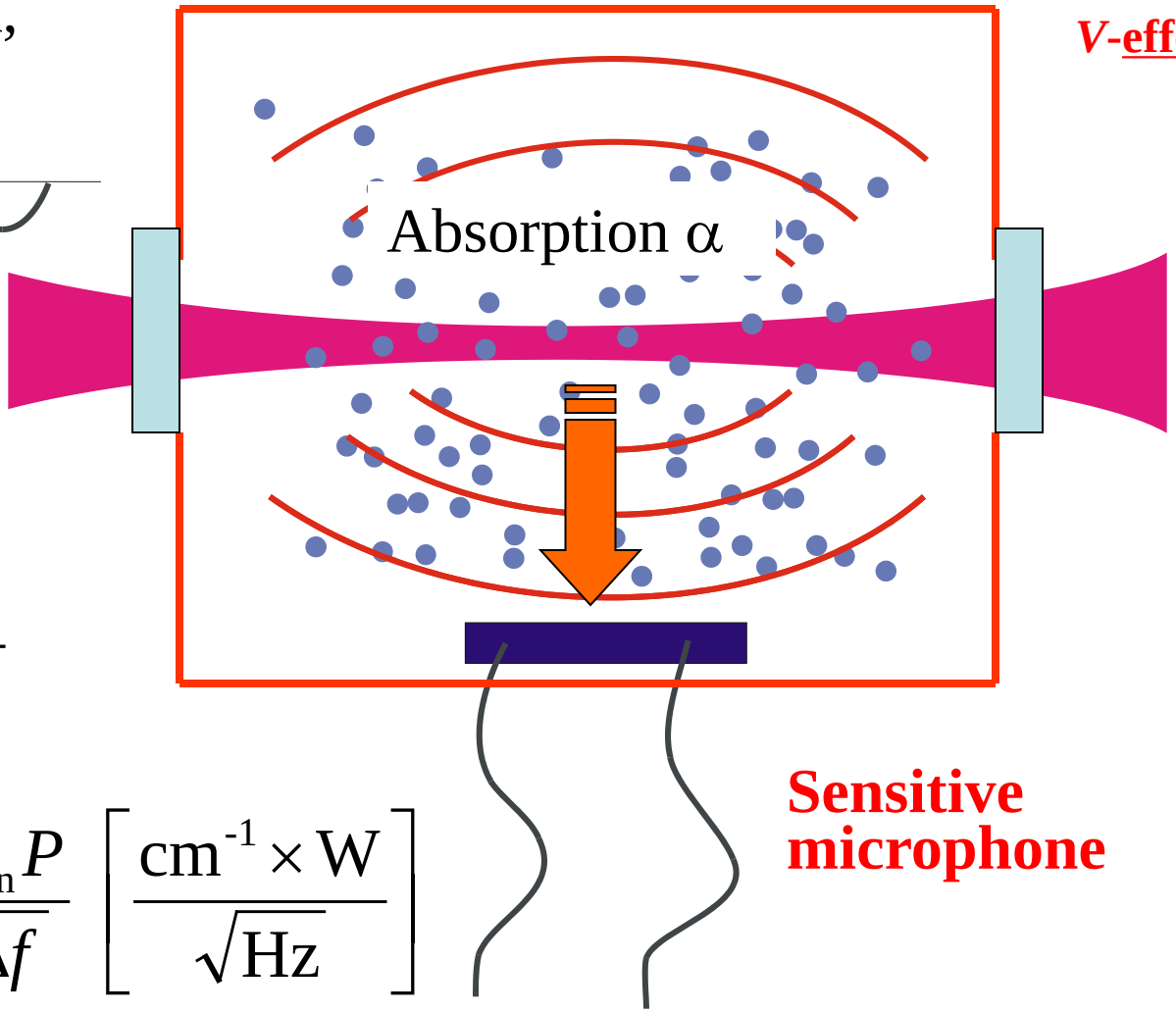

$$S \sim \frac{Q \alpha P}{f V}$$

$$NNEA = \frac{\alpha_{min} P}{\sqrt{\Delta f}} \left[\frac{cm^{-1} \times W}{\sqrt{Hz}} \right]$$

RICE

NH_3 Measurements based on an EC-QCL PAS Sensor System

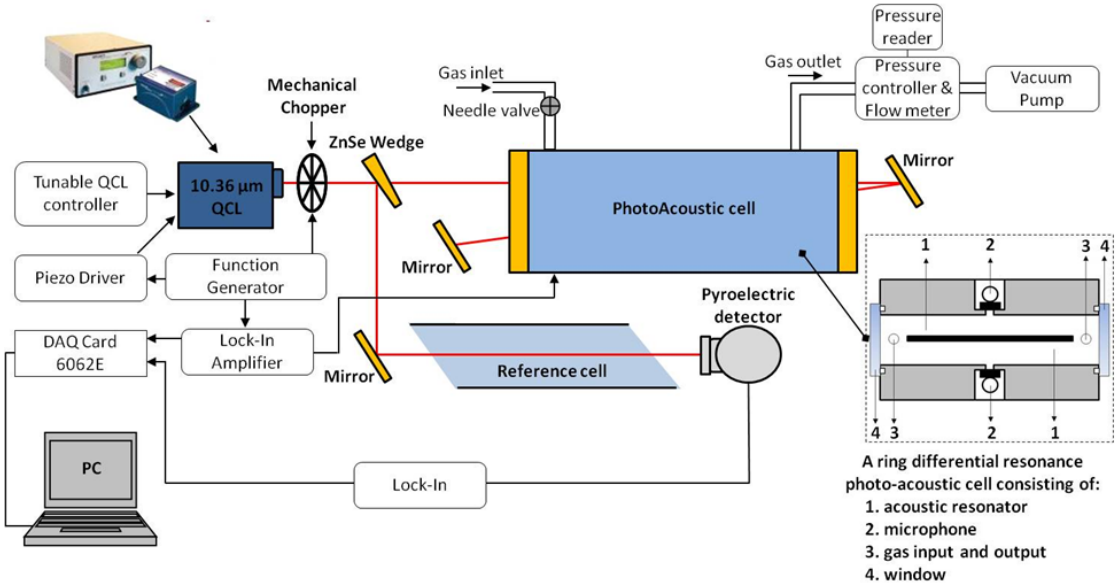

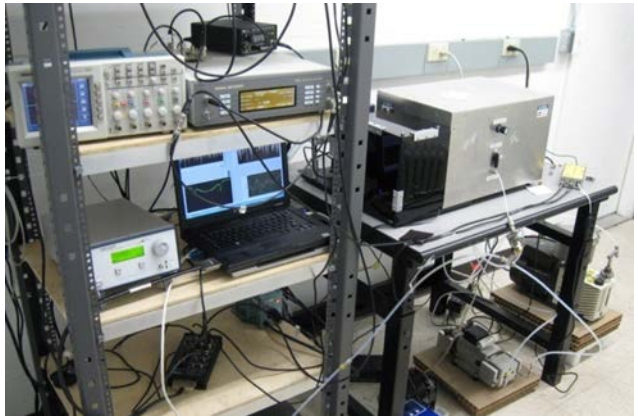

NH_3 sensor deployed at the UH Moody Tower rooftop monitoring site.

Schematic of a Daylight Solutions 10.36 µm CW TEC EC-QCL based PAS NH_3 Sensor.

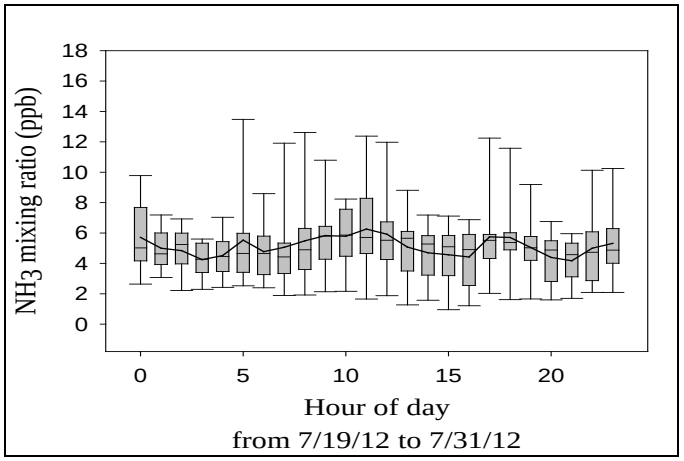

Diurnal profile of atmospheric NH_3 levels in Houston, TX.

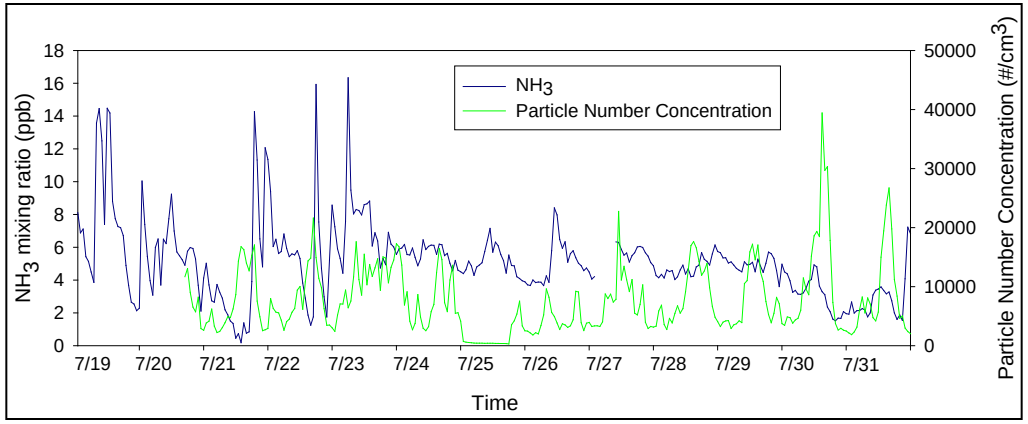

Comparison between NH_3 and particle number concentration time series from July 19 to July 31 2012.

Unexpected Remote Detection of NH_3 based on PAS

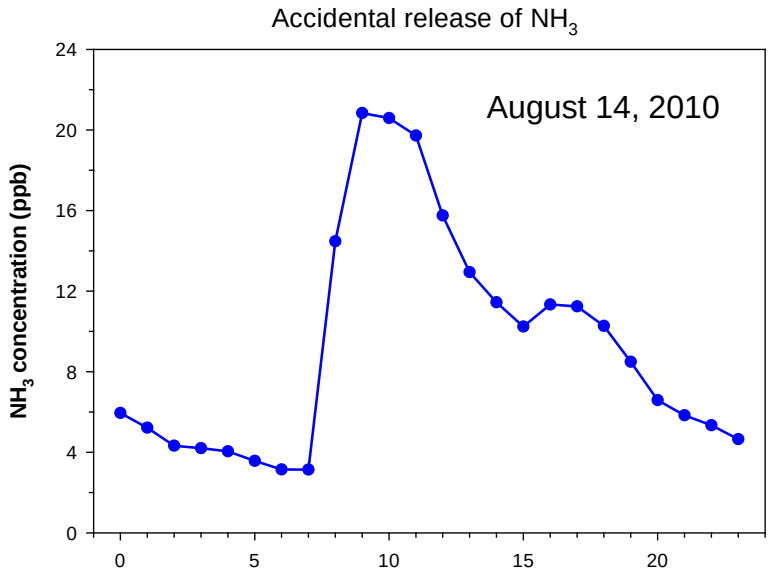

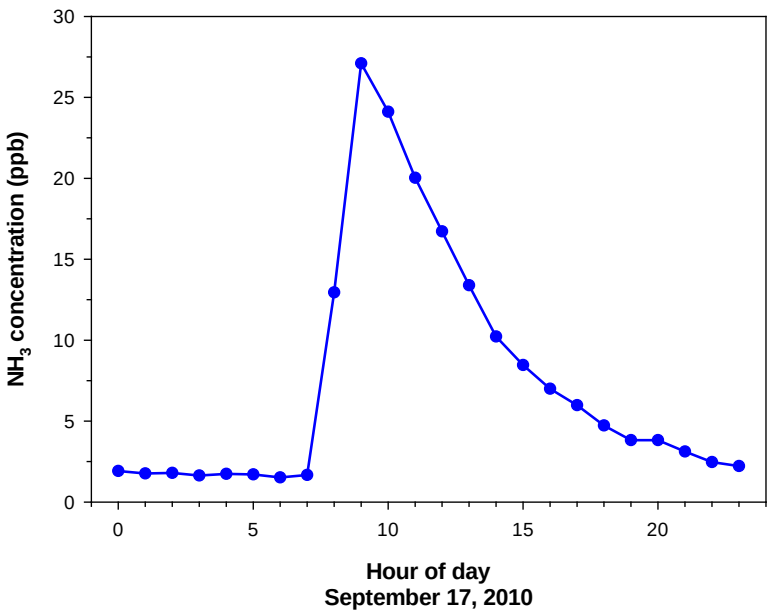

A chemical incident occurred at ~ 6 a.m. after two trucks collided on I-59. Both trucks caught fire. [www.chron.com]

Estimated hourly NH_3 emission from the Houston Ship Channel area is about 0.25 ton. Mellqvist et al., (2007) Final Report, HARC Project H-53.

RICE

Remote Detection of Sporadic NH_3 Emissions from the Parish Electric Power Plant, TX

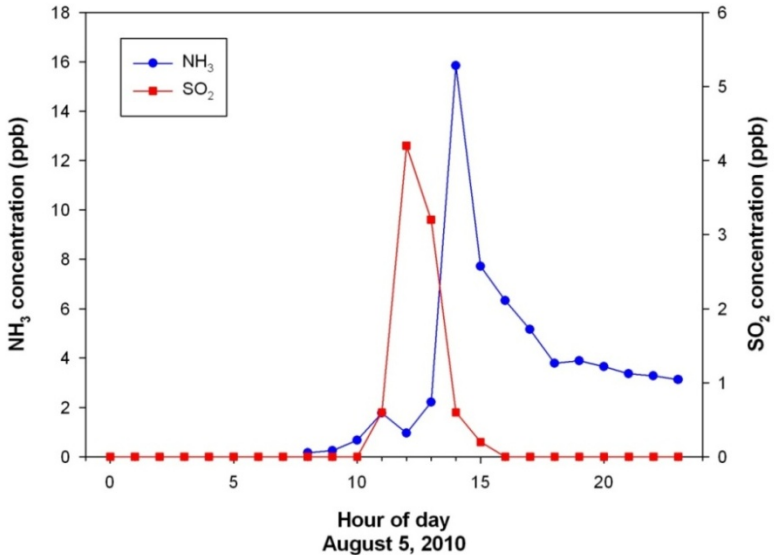

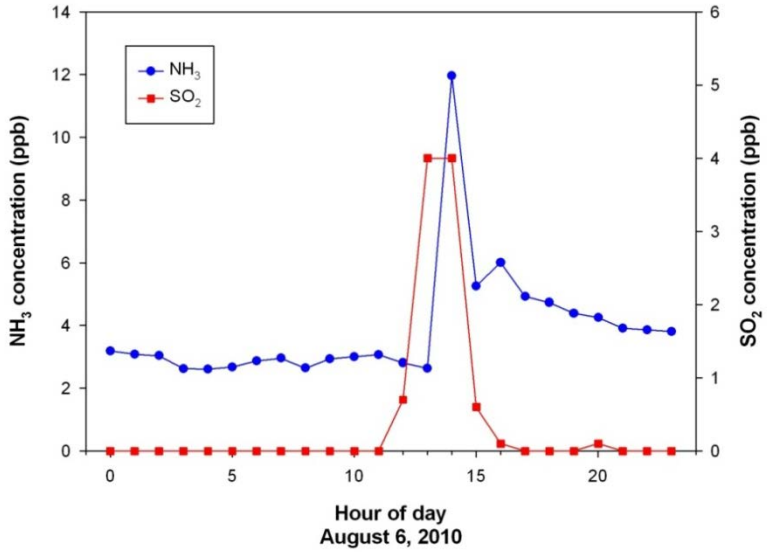

The Parish electric power plant is located near the Brazos River in Fort Bend County, Texas (~27 miles SW from downtown Houston)

RICE

Fort-Worth, Dallas(TX) CAMS 75 & TCEQ Monitoring Site

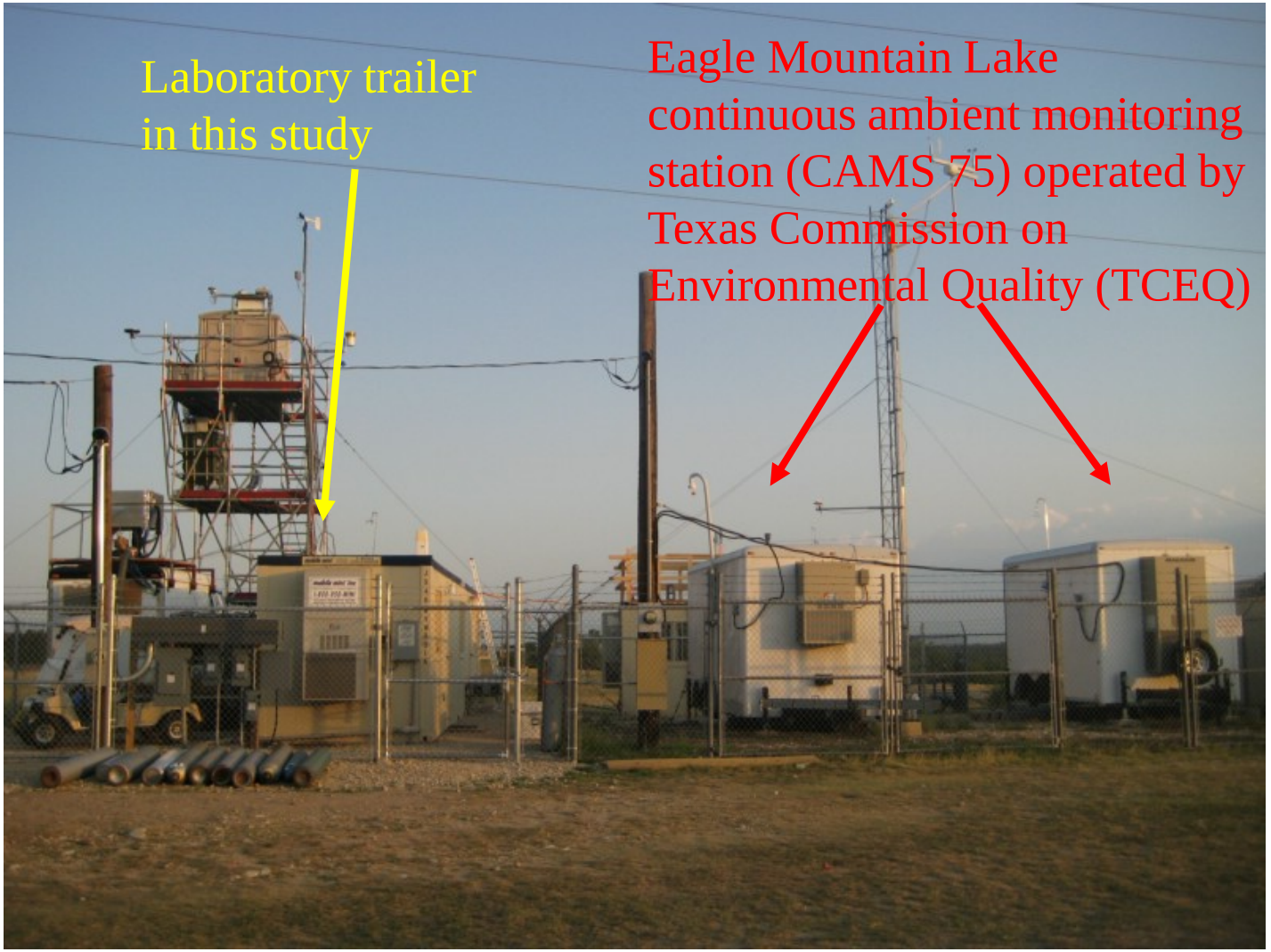

RICE

Available Instrumentation at CAMS 75 & TCEQ Monitoring Site

Species/parameter	Measurement technique
NH_3	Daylight Solutions External Cavity Quantum Cascade Laser (Photo-acoustic Spectroscopy)
CO	Thermo Electron Corp. 48C Trace Level CO Analyzer (Gas Filter Correlation)
SO_2	Thermo Electron Corp. 43C Trace Level SO_2 Analyzer (Pulsed Fluorescence)
NO_x	Thermo Electron Corp. 42C Trace Level NO-NO_2-NO_X Analyzer (Chemiluminescence)
NO_y	Thermo Electron Corp. 42C-Y NO_Y Analyzer (Molybdenum Converter)
HNO_3	Mist Chamber coupled to Ion Chromatography (Dionex, Model CD20-1)
HCl	Mist Chamber coupled to Ion Chromatography (Dionex, Model CD20-1)
VOC_s	IONICON Analytik Proton Transfer Reaction Mass Spectrometer and TCEQ Automated Gas Chromatograph
PBL height	Vaisala Ceilometer CL31 with updated firmware to work with Vaisala Boundary Layer View software
Temperature	Campbell Scientific HMP45C Platinum Resistance Thermometer
Wind speed	Campbell Scientific 05103 R. M. Young Wind Monitor
Wind direction	Campbell Scientific 05103 R. M. Young Wind Monitor

RICE

NH_3 Source Attribution & Temperature Variations

- Emission events from specified point sources (i.e., industrial facilities)
- Estimated NH_3 emissions from cows (1.3 tons/day)
- Estimated NH_3 emissions from soil and vegetation (0.15 tons/day)
- EPA PMF (biogenic:74.1%; light duty vehicles:12.1%; natural gas/industry: 9.4%; heavy duty vehicles:4.4%)
- Livestock might account for approximately 66.4% of total NH_3 emissions
- Increased contribution from industry (→18.9%)

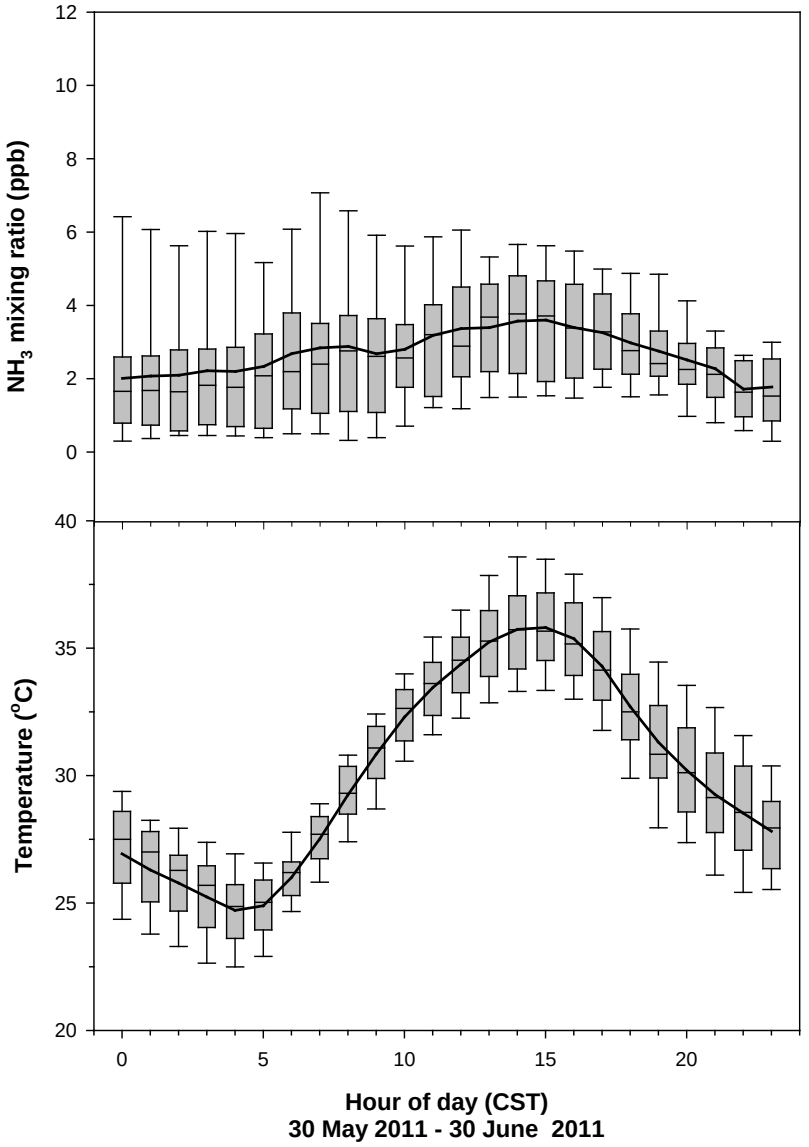

From Conventional **PAS** to Quartz Enhanced PAS (**QEPAS**)

Q>>1000

Cell is OPTIONAL!

***V*-effective volume**

Laser beam, power *P*

Modulated (*P* or λ) at *f* or *f*/2

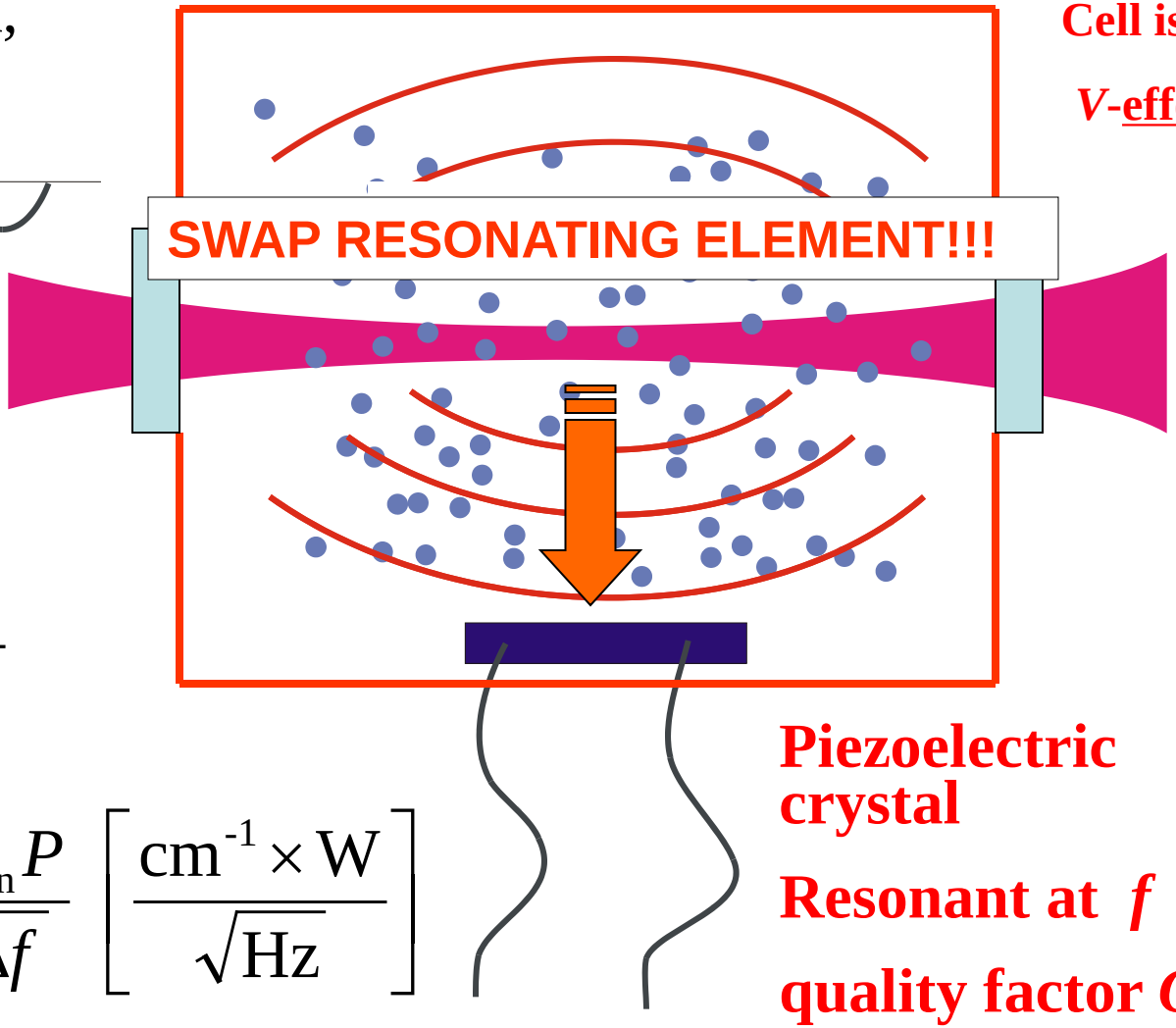

$$S \sim \frac{Q \alpha P}{f V}$$

$$NNEA = \frac{\alpha_{min} P}{\sqrt{\Delta f}} \left[\frac{cm^{-1} \times W}{\sqrt{Hz}} \right]$$

Piezoelectric crystal

Resonant at *f*

quality factor *Q*

RICE

Quartz Tuning Fork as a Resonant Microphone for QEPAS

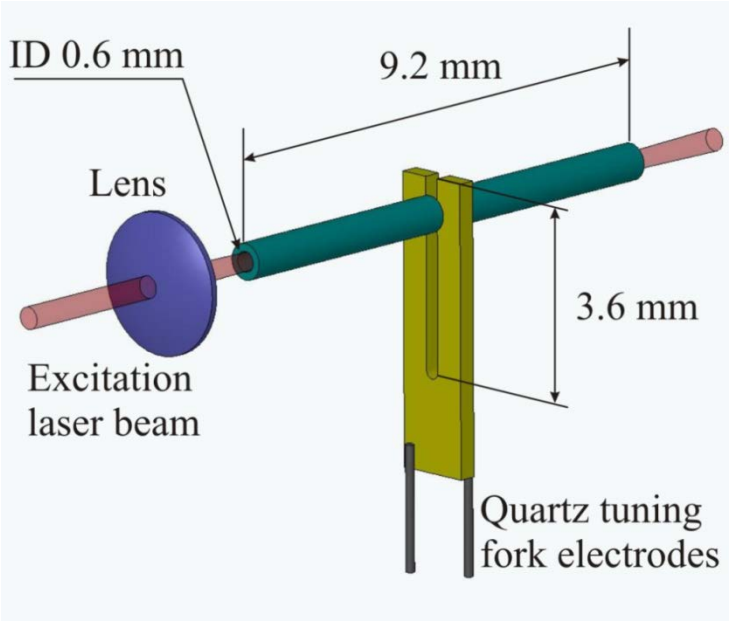

Unique Properties

- Extremely low internal losses:
  - Q~10 000 at 1 atm
  - Q~100 000 in vacuum
- Acoustic quadrupole geometry
  - Low sensitivity to external sound
- Large dynamic range (~10^6) – linear from thermal noise to breakdown deformation
  - 300K noise: x~10^{-11} cm
  - Breakdown: x~10^{-2} cm
- Wide temperature range: from 1.6K to ~700K

Acoustic Micro-resonator (μR) Tubes

- Optimum inner diameter: 0.6 mm; μR-QTF gap is 25-50 μm
- Optimum mR tubes must be ~ 4.4 mm long (~$\lambda/4<l<\lambda/2$ for sound at 32.8 kHz)
- SNR of QTF with μR tubes: ×30 **(**depending on gas composition and pressure)

Optimum NH_3 Line Selection for a 10.34 μm CW TEC DFB QCL

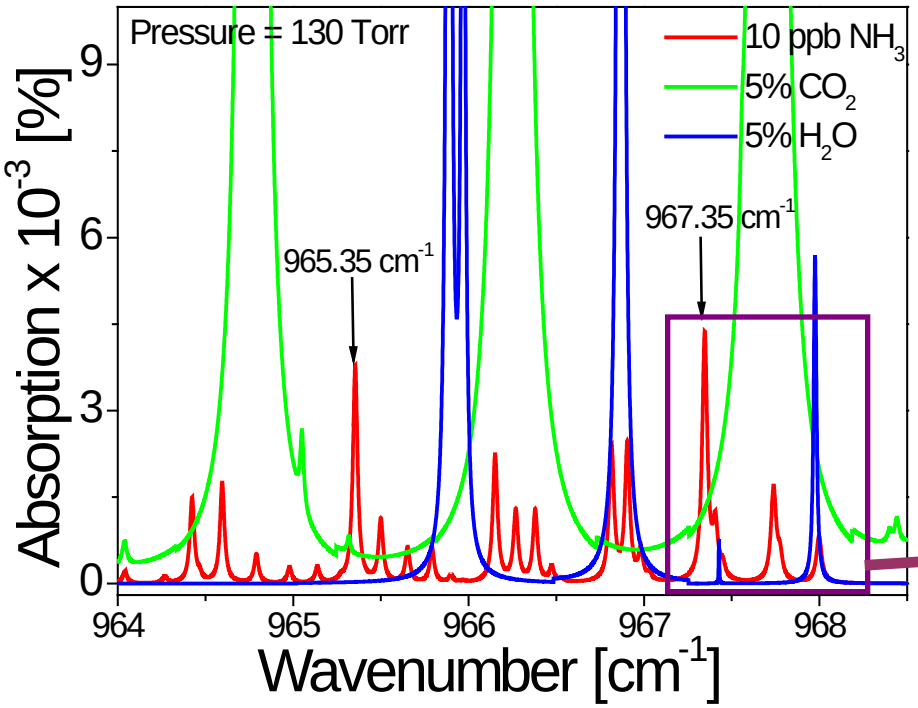

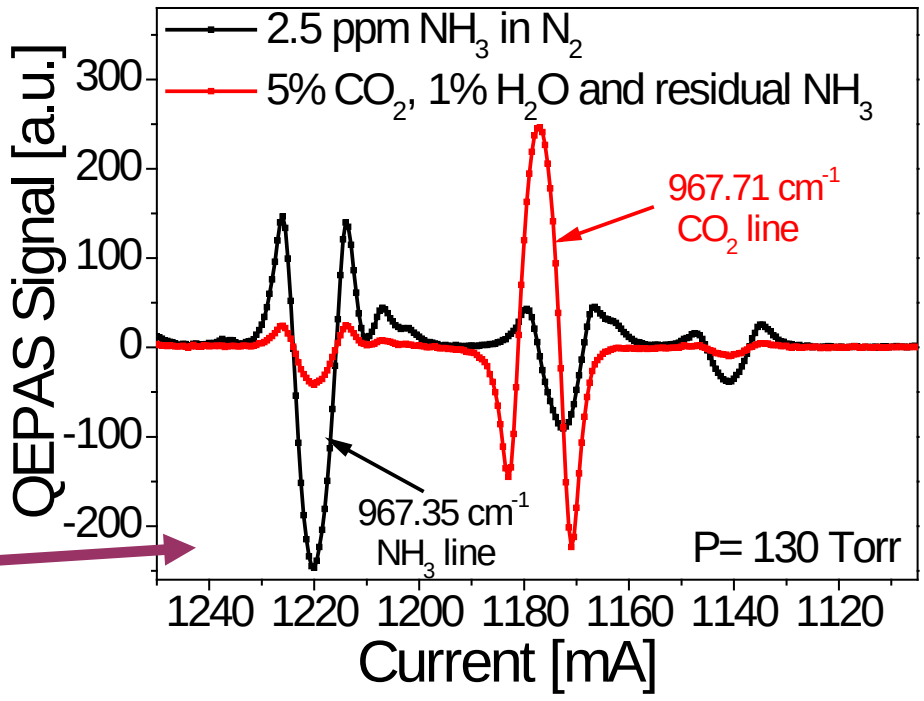

Simulated HITRAN high resolution spectra @ 130 Torr indicating two NH_3 absorption lines of interest

No overlap between NH_3 and CO_2 absorption lines was observed for the selected **967.35 cm^{-1}** NH_3 absorption line in the ν_2 R-band.

RICE

QEPAS based NH_3 Gas Sensor Architecture

Loccioni breath sampler

Gas handling system

Diaphragm Pump

To the system

Tee connector

Needle valve

Pressure Controller & Flow Meter

Gas In

Gas Out

Mouth piece & Capnostat

Mid-IR DFB-QCL

Current & Temp controller

Lenses

ADM

Reference Cell

Pyroelectric detector

Pre-Amp

DAQCard 6062E

Lock-In 2f

Lock-In 3f

Data collection and processing

PC

Control Electronics Unit (CEU)

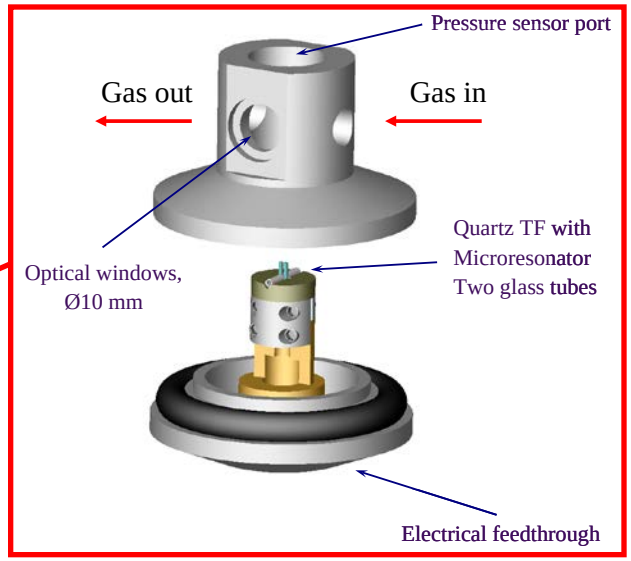

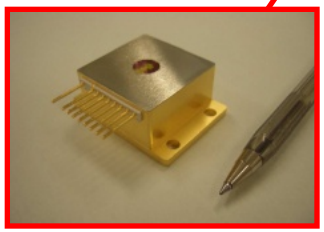

CW TEC DFB QCL in HHL package (Hamamatsu)

RICE

Real-time Exhaled Human NH_3 Breath Measurements

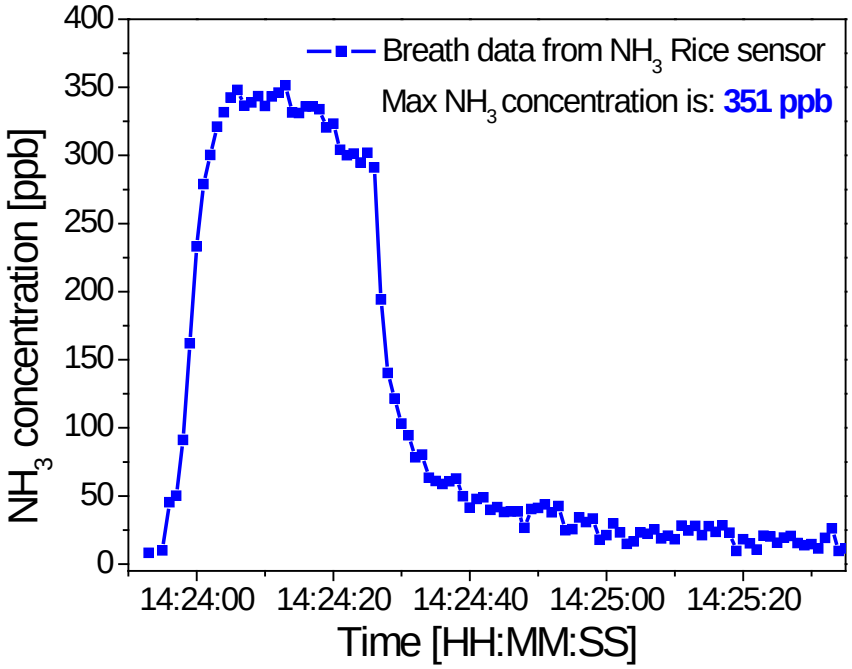

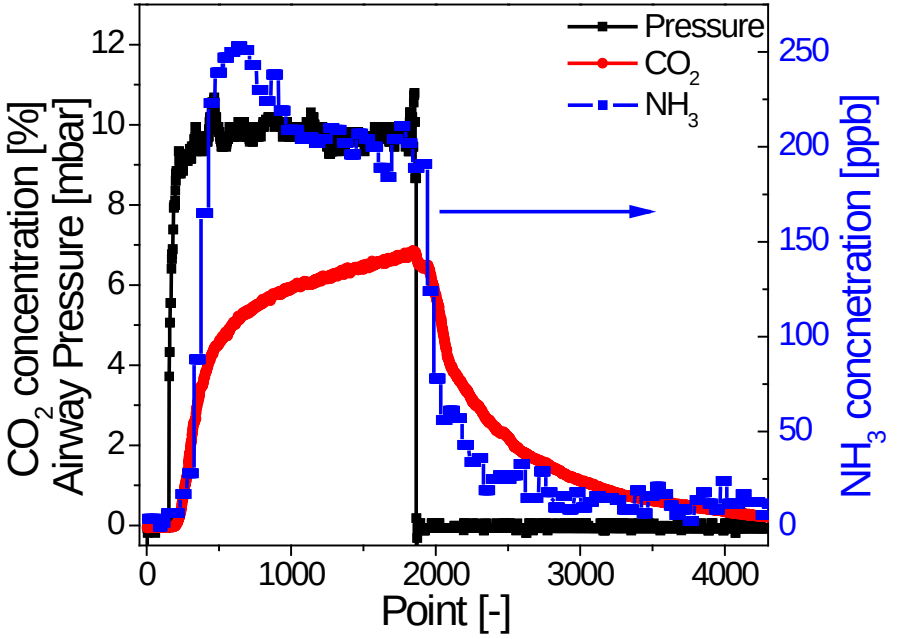

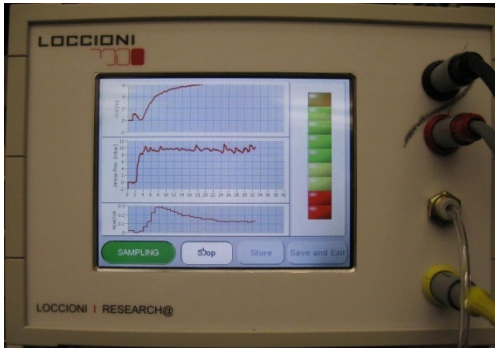

Airway pressure (black), CO_2 (red), and NH_3 (blue) profiles of a single breath exhalation lasting 40sec.

Successful testing of a 2nd generation breath ammonia monitor installed in a clinical environment.(Johns Hopkins, Baltimore, MD and St. Luke's Hospital, Bethlehem, PA)

Minimum detectable concentration of NH_3 is:
~ 6 ppbv at 967.35 cm^{-1} (1σ; 1 s time resolution)

Motivation for Nitric Oxide Detection

- **NO in medicine and biology**
  - Important signaling molecule in physiological processes in humans and mammals (1998 Nobel Prize in Physiology/Medicine)
  - Treatment of asthma, chronic obstructive pulmonary disease (COPD) & lung rejection
- **Environmental pollutant gas monitoring**
  - Ozone depletion
  - Precursor of smog and acid rain
  - NO_X monitoring from automobile exhaust and power plant emissions
- **Atmospheric Chemistry**

RICE

Molecular Absorption Spectra within two Mid-IR Atmospheric Windows and NO absorption @ 5.26µm

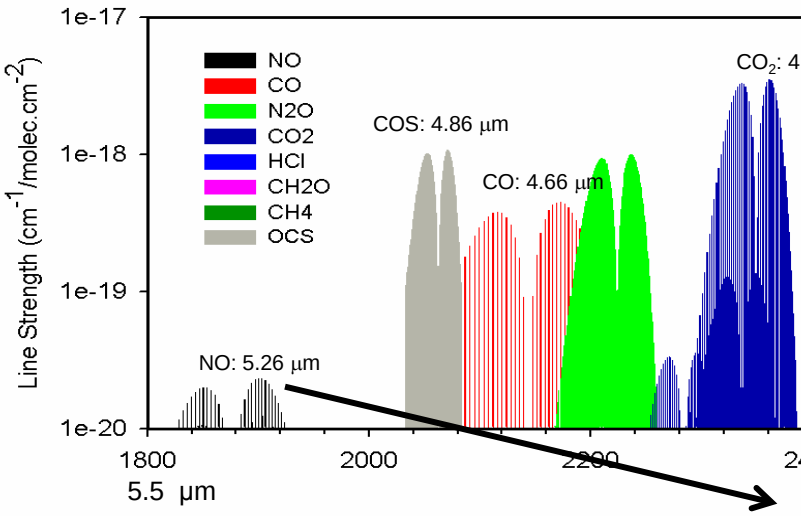

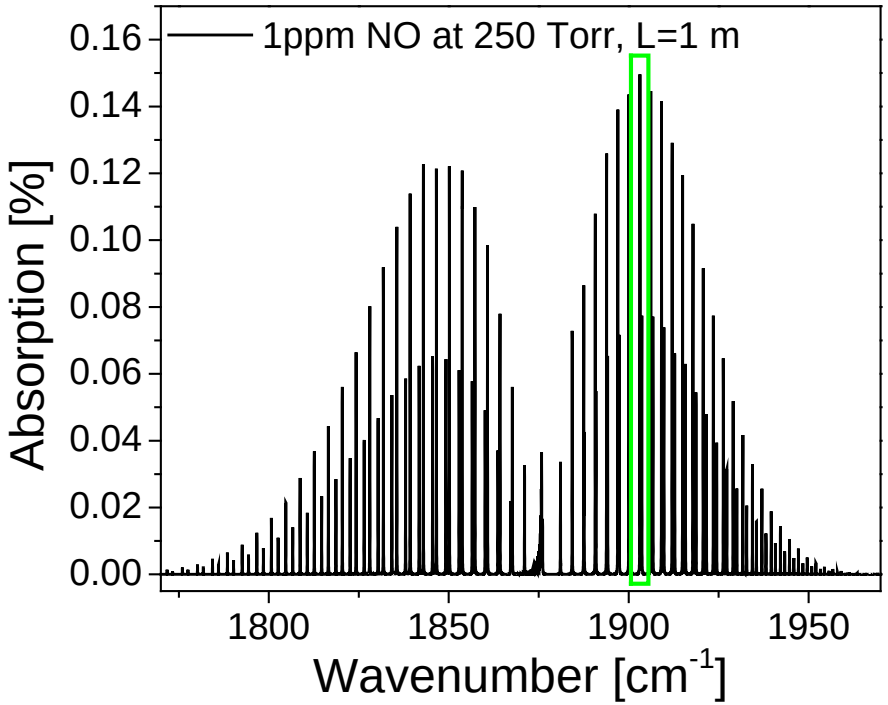

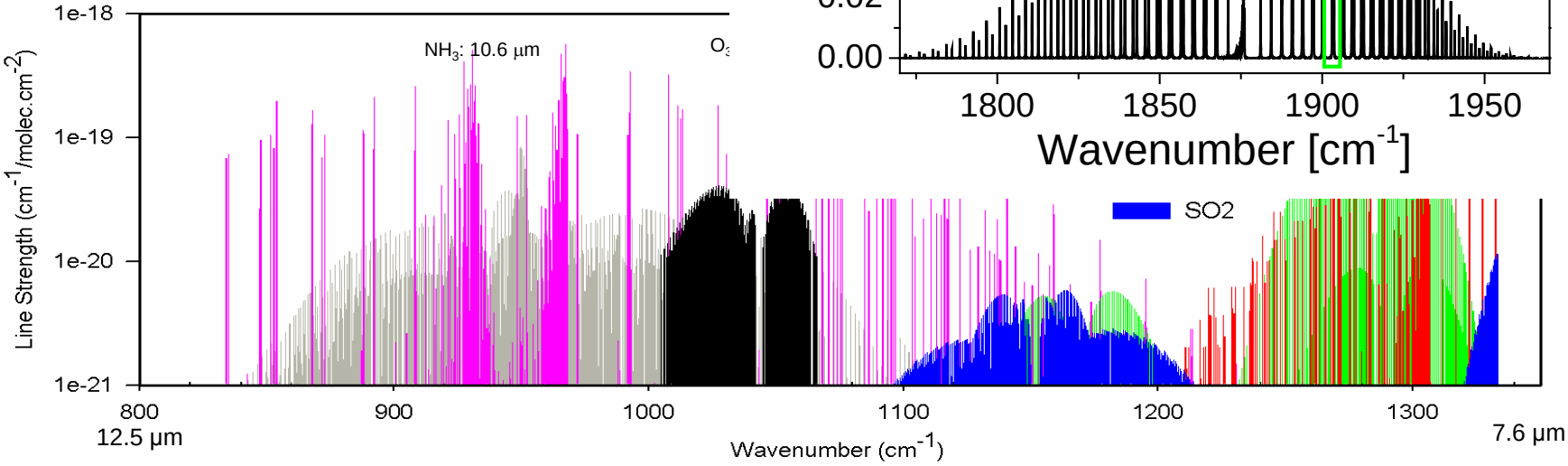

Source: HITRAN 2012 database

RICE

Emission Spectra of a 1900cm^{-1} TEC DFB QCL and HITRAN simulated spectra of NO, H_2O & CO_2

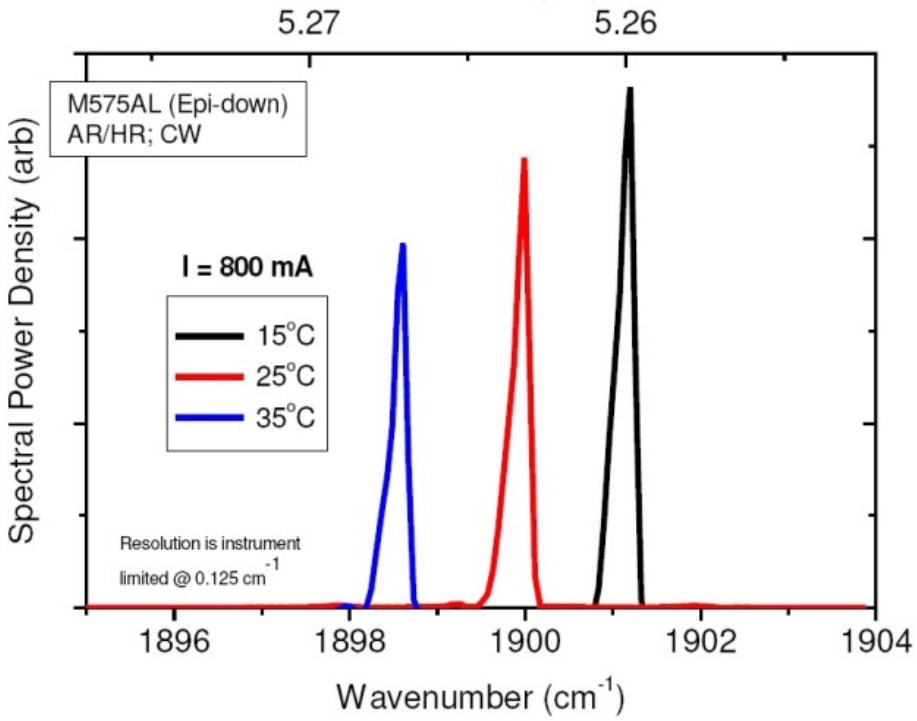

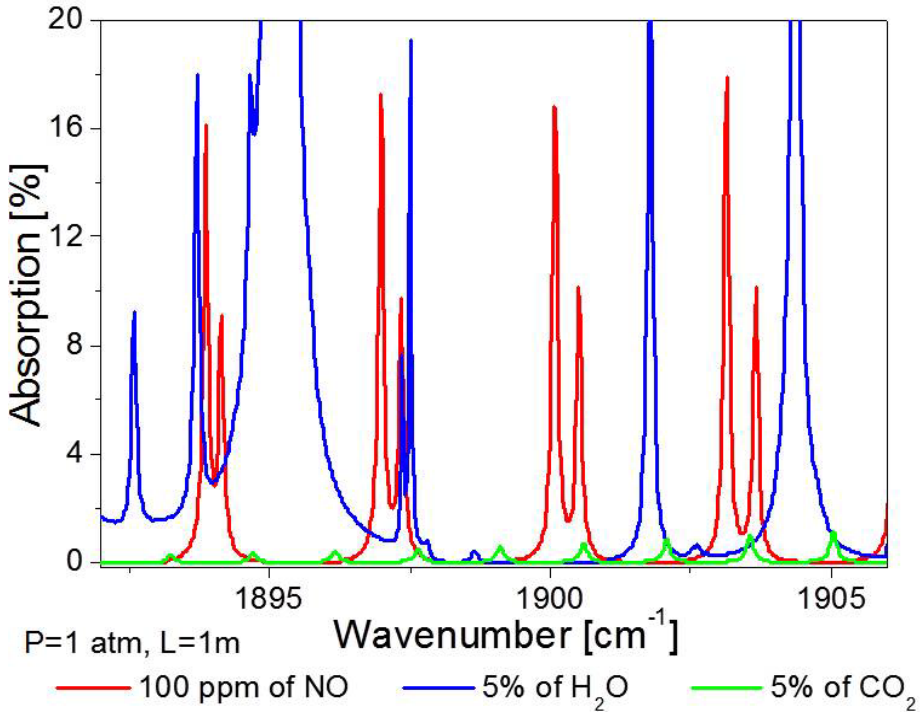

Output power: 117 mW @ 25 C
Thorlabs/Maxion

RICE

Performance of a 5.26 μm CW HHL TEC DFB-QCL

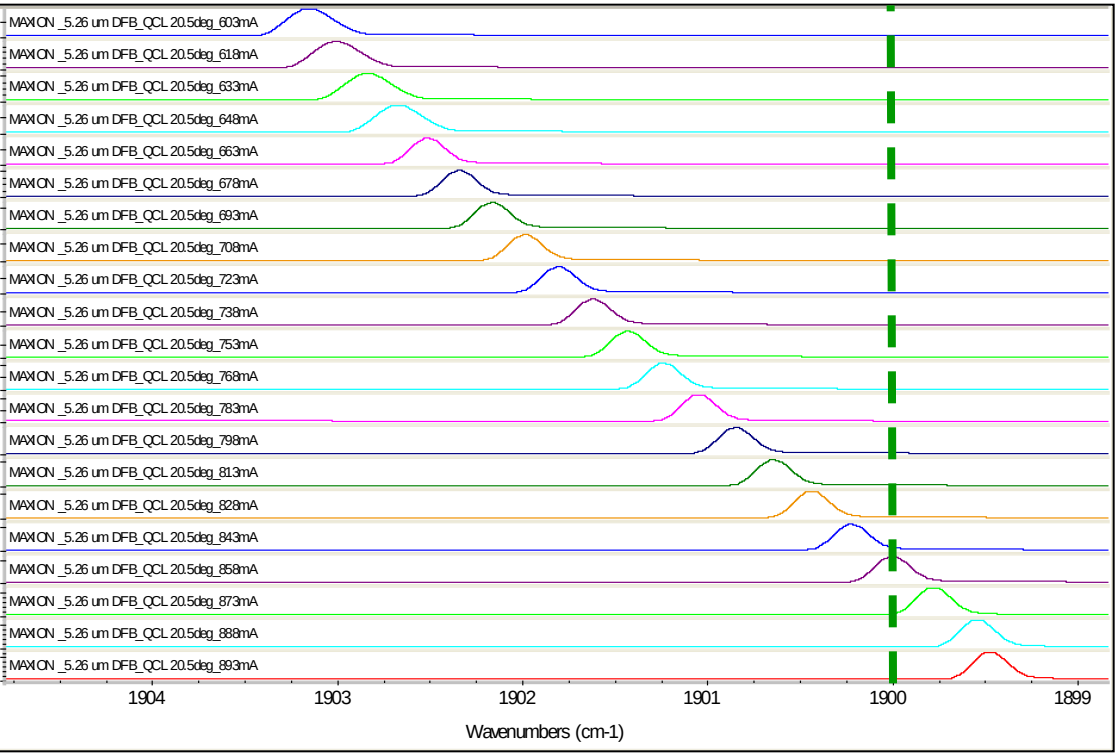

Single frequency QCL radiation recorded with FTIR for different laser current values at a QCL temperature of 20.5°C.

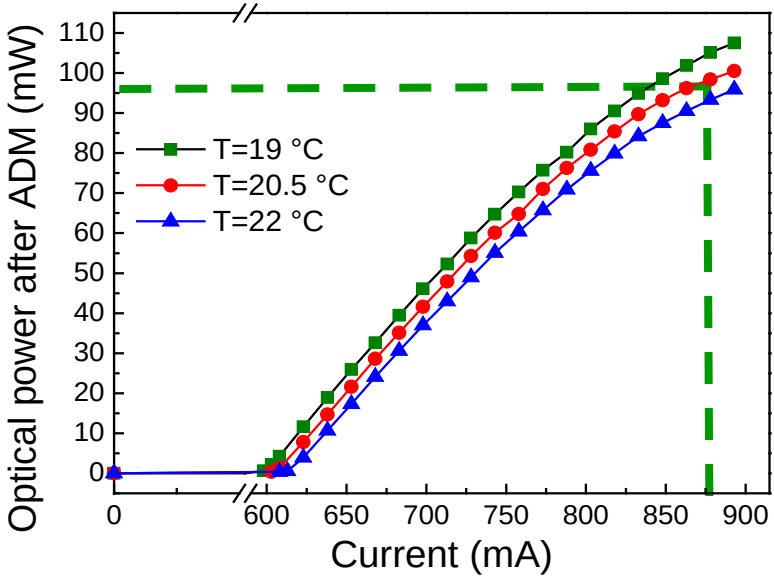

CW DFB-QCL optical power and current tuning at three different temperatures.

RICE

CW TEC DFB QCL based QEPAS NO Gas Sensor

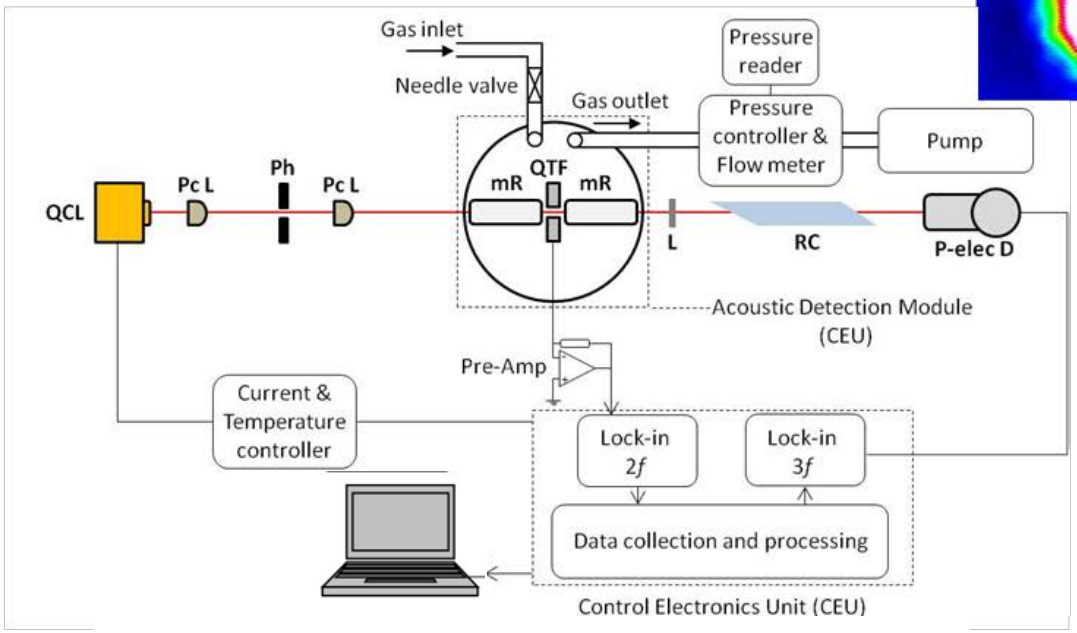

Schematic of a DFB-QCL based Gas Sensor.
PcL – plano-convex lens, Ph – pinhole,
QTF – quartz tuning fork, mR – microresonator,
RC- reference cell, P-elec D – pyro electric detector

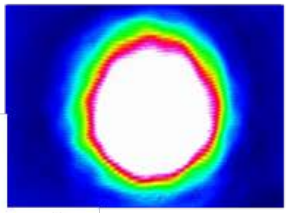

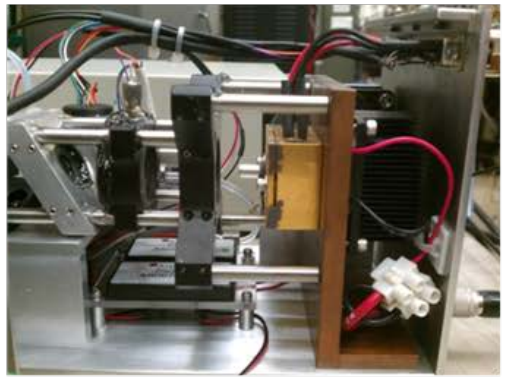

CW HHL TEC DFB-QCL package and IR camera image of the laser beam at 630 mA and 20.5 deg C through tubes after ADM

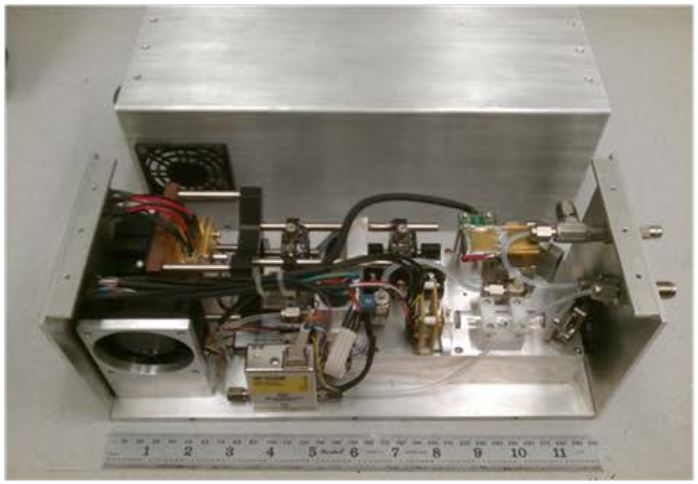

Compact Prototype NO Sensor (September 2012)

RICE

Performance of CW DFB-QCL based WMS QEPAS NO Sensor Platform

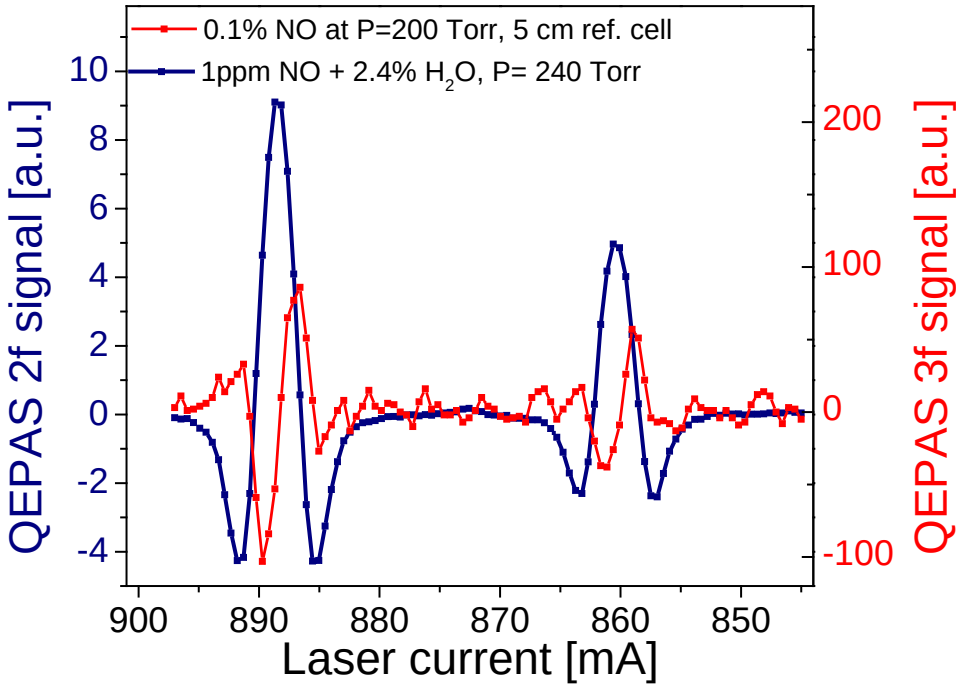

2f QEPAS signal (navy) and reference 3f signal (red) when DFB-QCL was tuned across **1900.08 cm^{-1}** NO line.

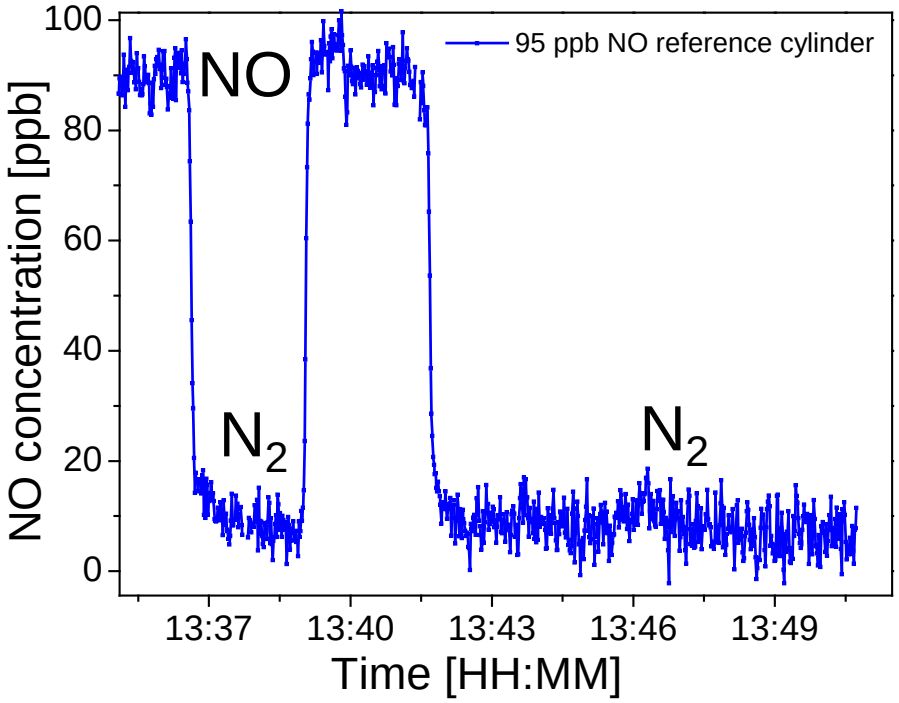

2f QEPAS signal amplitude for 95 ppb NO when DFB-QCL was locked to the **1900.08 cm^{-1}** line.

Minimum detectable NO concentration is:

~ 3 ppbv (1σ; 1 s time resolution)

RICE

QCL based TDLAS Sensor for Detection of NO Emission from Cancer Cells

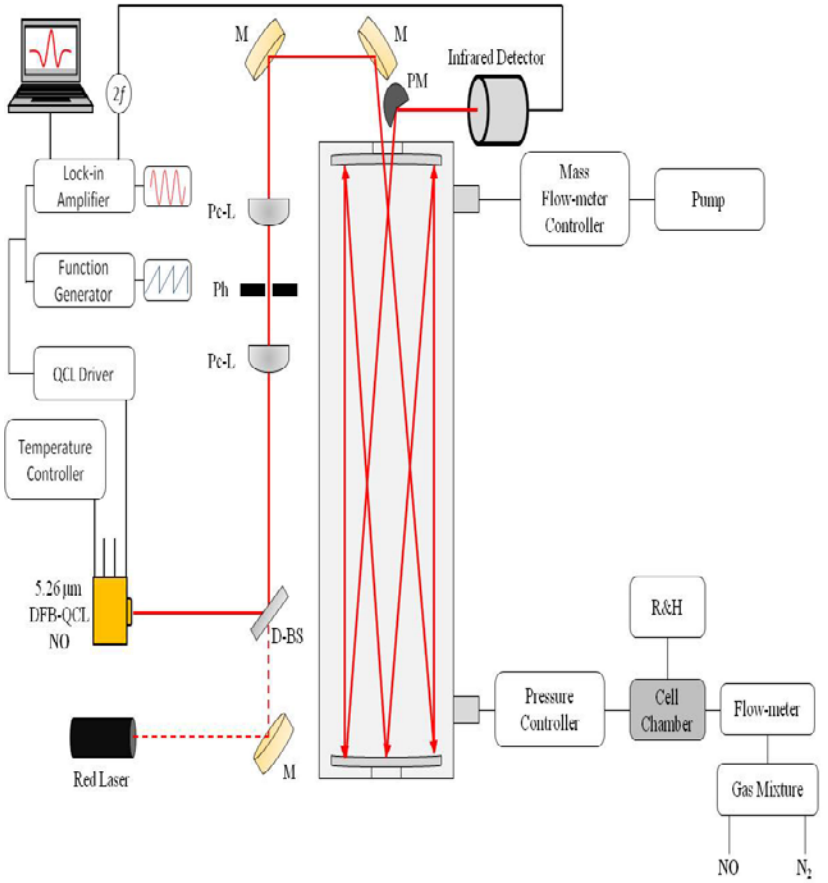

Schematic drawing of the sensor setup

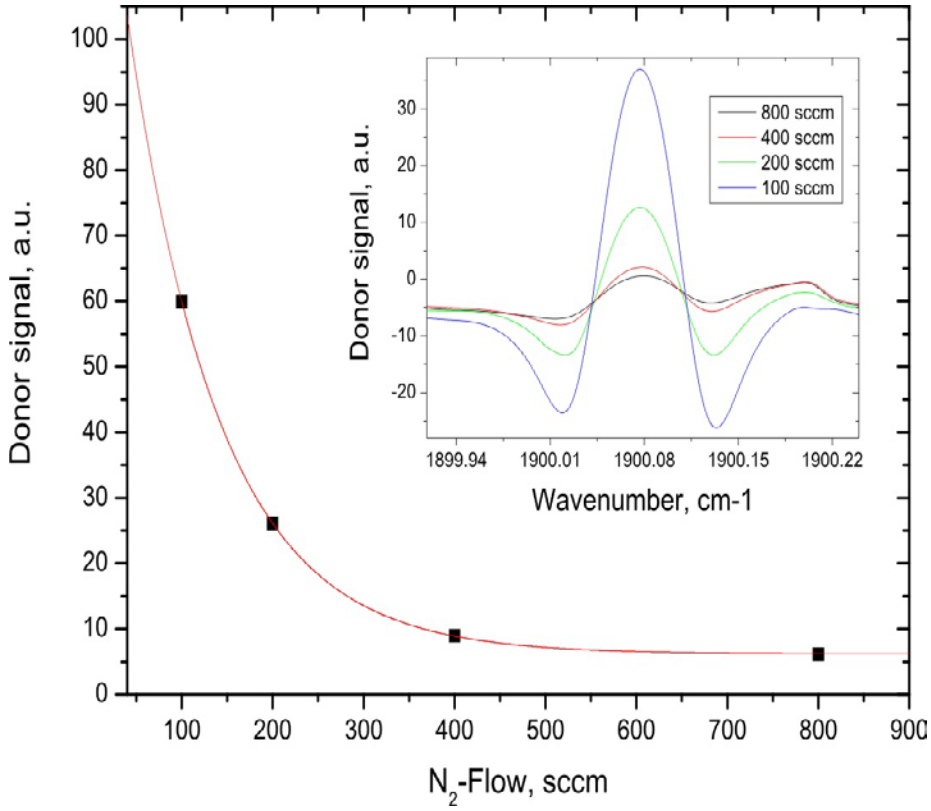

Dependence of the TDLAS sensor signal from biological samples on the gas flow (black squares). The inset shows spectra corresponding to the data points.

M.Koehring et al, Appl. Phys B , May 2014

Motivation for Carbon Monoxide Detection

- **CO in Medical Diagnostics**
  - Hypertension and abnormality in heme metabolism
- **Public Health**
  - Extremely dangerous to human life even at a low concentrations. CO must be monitored at low concentration levels (<35 ppm).
- **Atmospheric Chemistry**
  - Incomplete combustion of natural gas, fossil fuel and other carbon containing fuels.
  - Impact on atmospheric chemistry through its reaction with hydroxyl (OH) for troposphere ozone formation and changing the concentration levels of greenhouse gases (e.g. CH_4).

RICE

Performance of a 4.61μm high power CW TEC DFB QCL

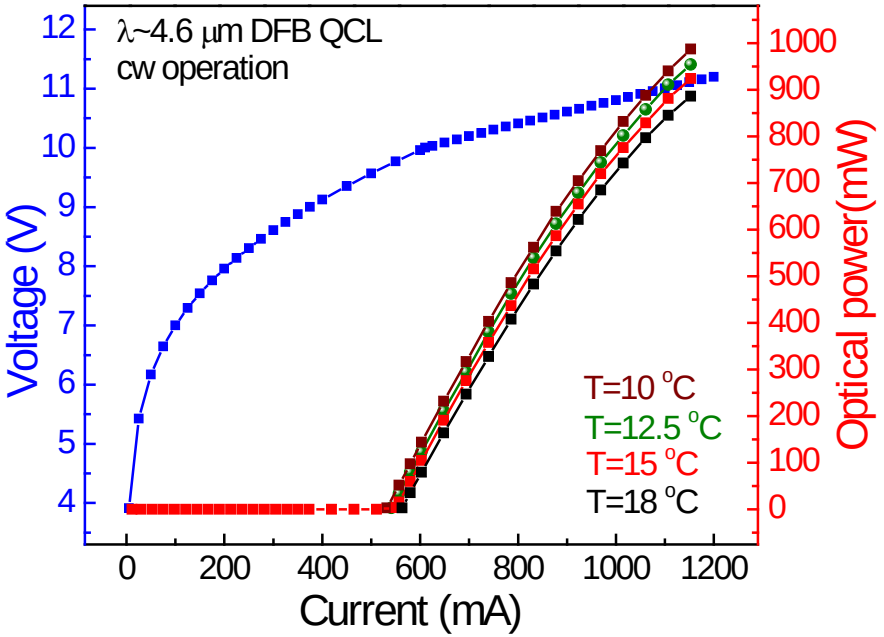

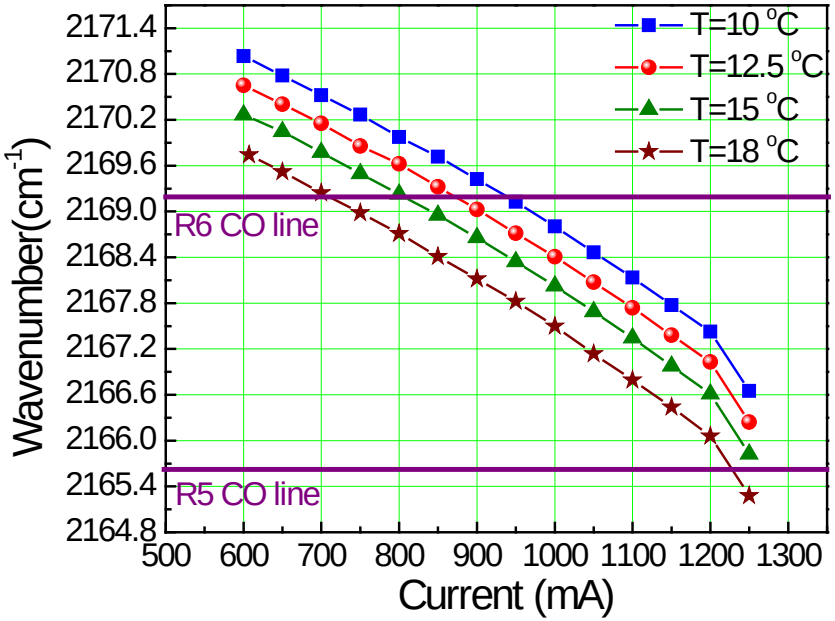

CW DFB-QCL optical power and current tuning at a four different QCL temperatures.

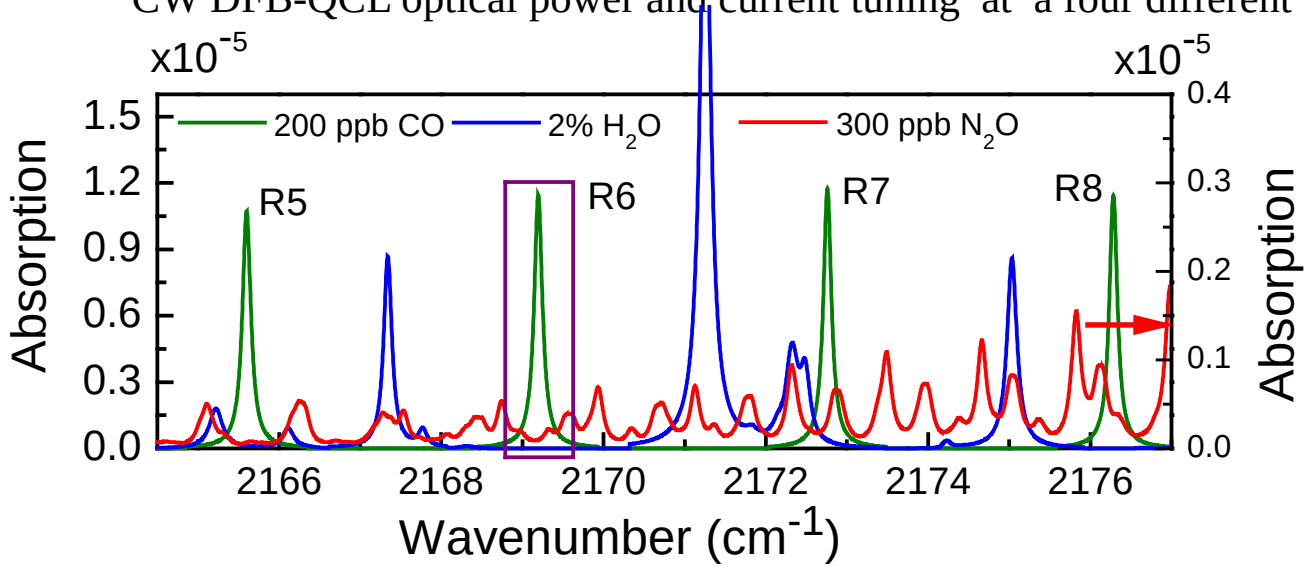

Estimated max wall-plug efficiency (WPE) is ~ 7% at 1.25A QCL drive-current.

RICE

CW DFB-QCL based CO QEPAS Sensor Results

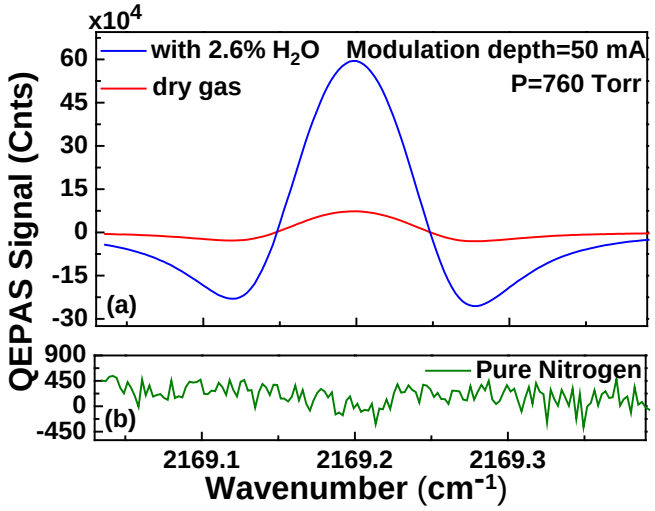

2f QEPAS signal for dry (red) and moisturized (blue) 5 ppm CO:N_2 mixture near **2169.2 cm^{-1}**.

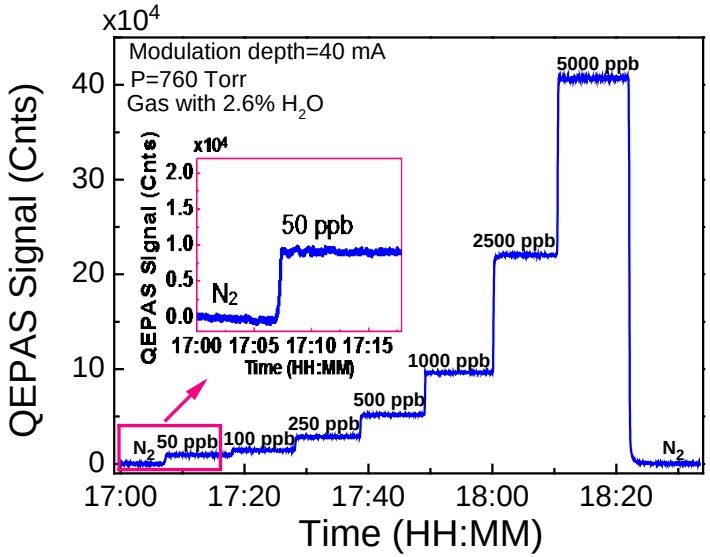

Dilution of a 5 ppm CO reference gas mixture when the CW DFB-QCL is locked to the **2169.2 cm^{-1}** R6 CO line.

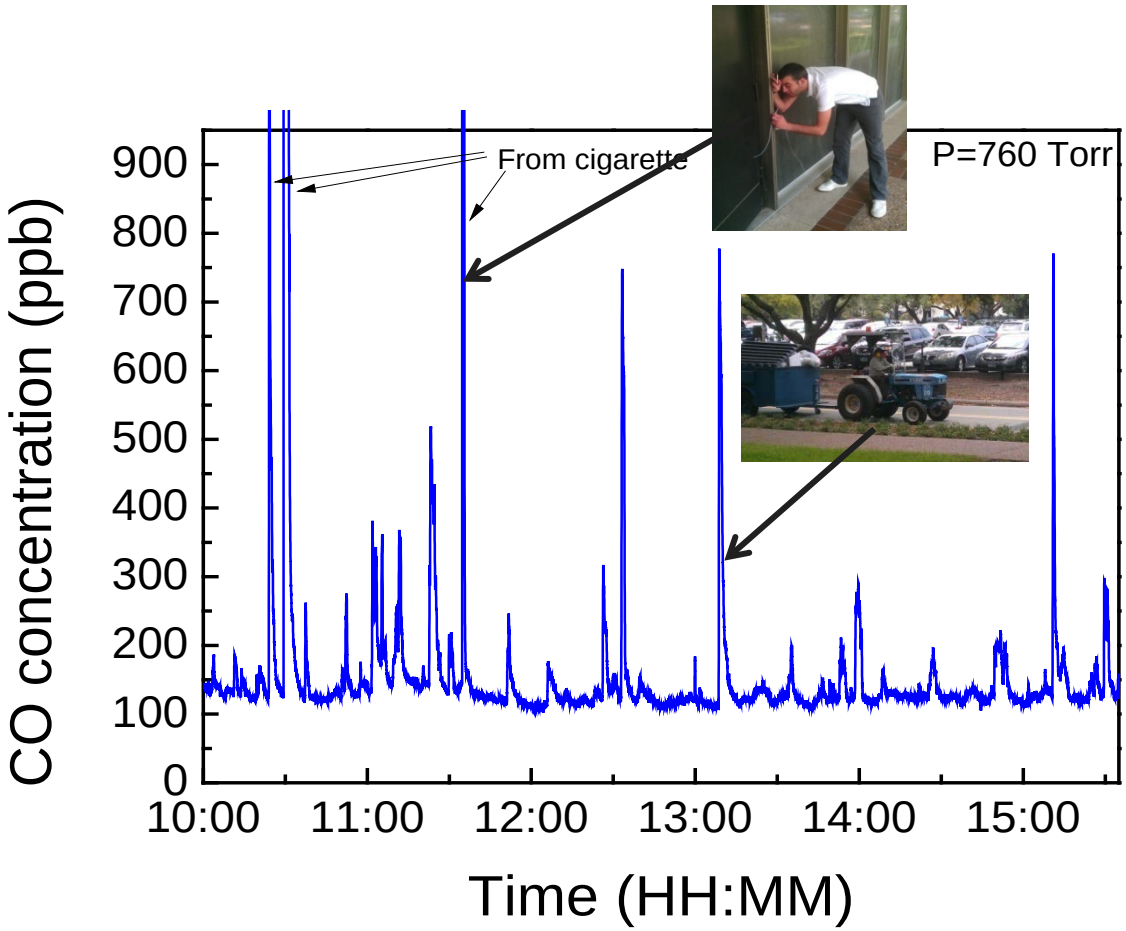

Atmospheric CO concentration levels on Rice University campus, Houston, TX

Minimum detectable CO concentration is:

~ 2 ppbv (1σ; 1 s time resolution)

P. Stefanski et al,, Appl. Phys. B,, June 3, 2014 (online)

RICE

CW DFB-QCL based SO_2 QEPAS Results

Motivation for Sulfur Dioxide Detection

- SO_2 exposure affects lungs and causes breathing difficulties, bronchitis, cardiovascular disease
- Currently, reported annual average atmospheric SO_2 concentrations range from ~ 1 - 6 ppb
- Prominent air pollutant
- Emitted from coal fired power plants (~73%) and other industrial facilities (~20%)
- In the atmosphere SO_2 converts to sulfuric acid ➔ primary contributors to acid rain
- SO_2 reacts to form sulfate aerosols
- Primary SO_2 exposure for 1 hour is 75 ppb

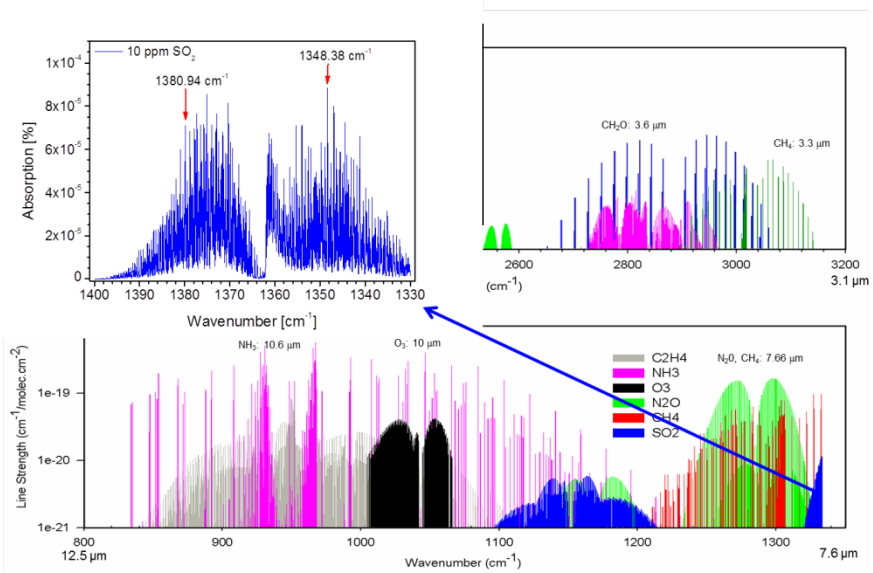

Molecular Absorption Spectra within two Mid-IR Atmospheric Windows

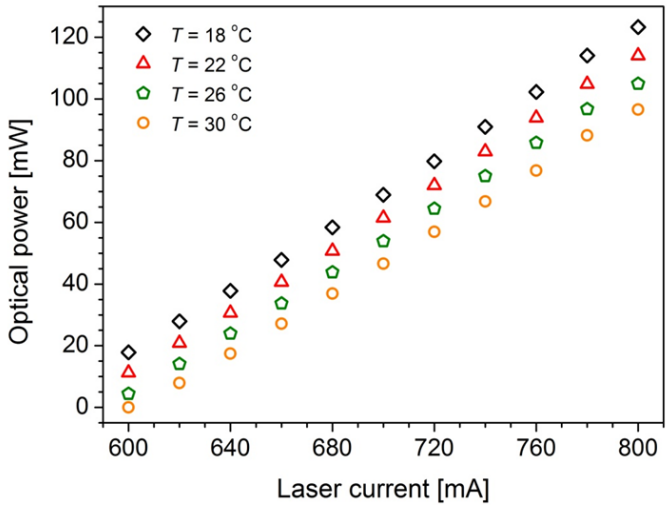

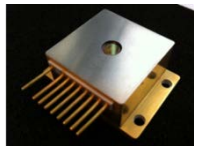

7.24 μm CW DFB-QCL optical power and current tuning at three different operating temperatures.

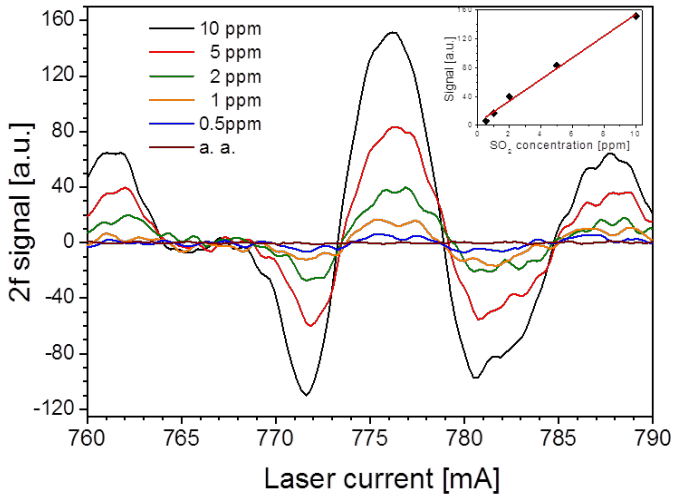

2f WMS QEPAS signals for different SO_2 concentrations when laser was tuned across **1380.9 cm^{-1}** line.

Minimum detectable SO_2 concentration is:
~ 100 ppbv (1σ; 1 s time resolution)

QEPAS based CH_4 and N_2O Gas Sensor

Motivation for CH_4 and N_2O Detection

- Medical Diagnostics
  - Nausea, blurred vision, vomiting
- Prominent greenhouse gases
- Sources: wetlands, leakage from natural gas systems, fossil fuel production and agriculture

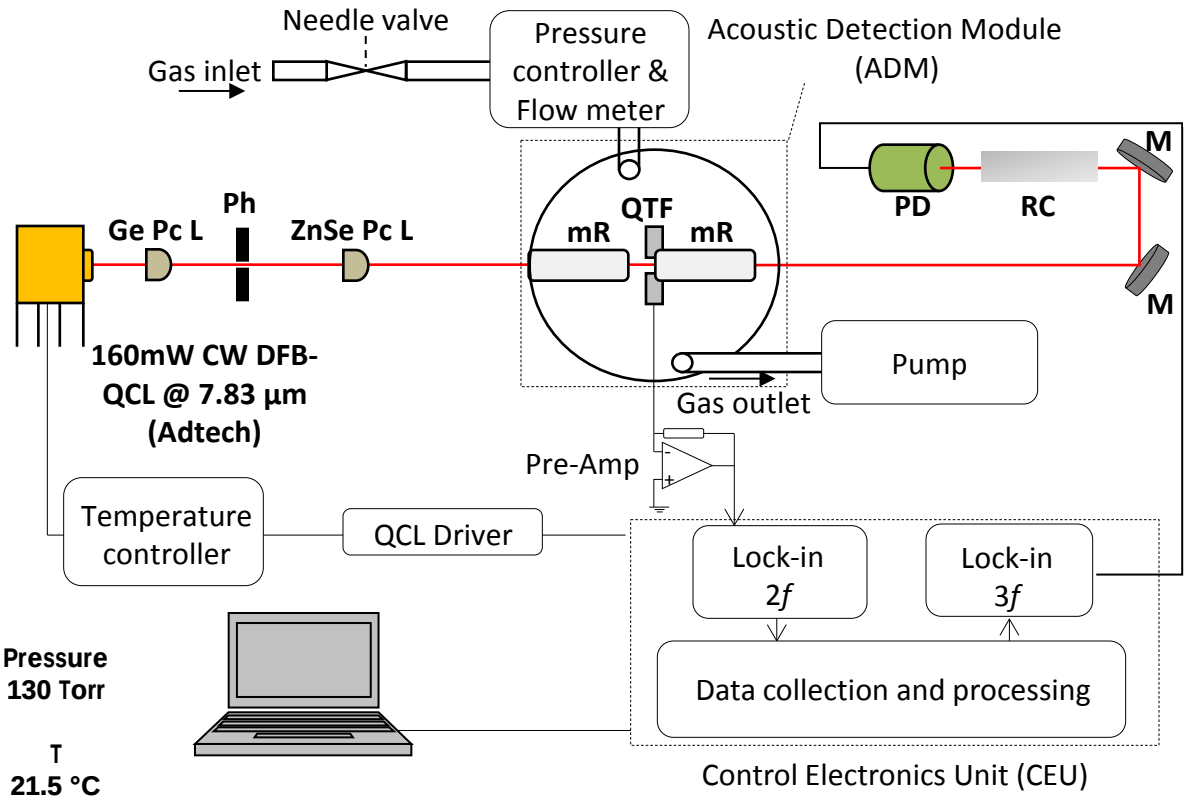

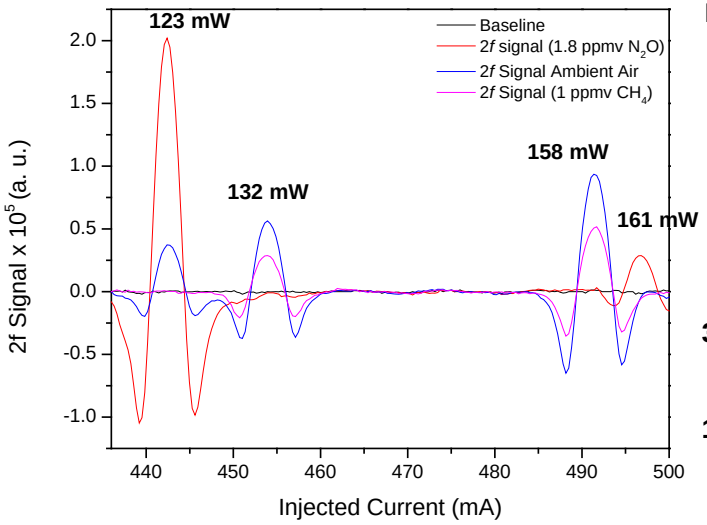

Pressure
130 Torr

T
21.5 °C

AM
4 mA

f
32760 Hz

f_{mod}
16380 Hz

Detection Limit (1σ) with a **1-sec** averaging time
Methane (CH_4) (1275.04 cm^{-1}) **13 ppbv**
Nitrous Oxide (N_2O) (1275.5 cm^{-1}) **6 ppbv**

N_2O concentration in the ambient laboratory air:
331 ppbv

M. Jahjah et al., Analyst, 139, 2063-2069, 2014 & Appl. Lett, 39, 957-960, 2014

RICE

CH_4 Measurements performed with a DFB-QCL based QEPAS Sensor installed in the Aerodyne Mobile Laboratory (Sept 7, 2013)

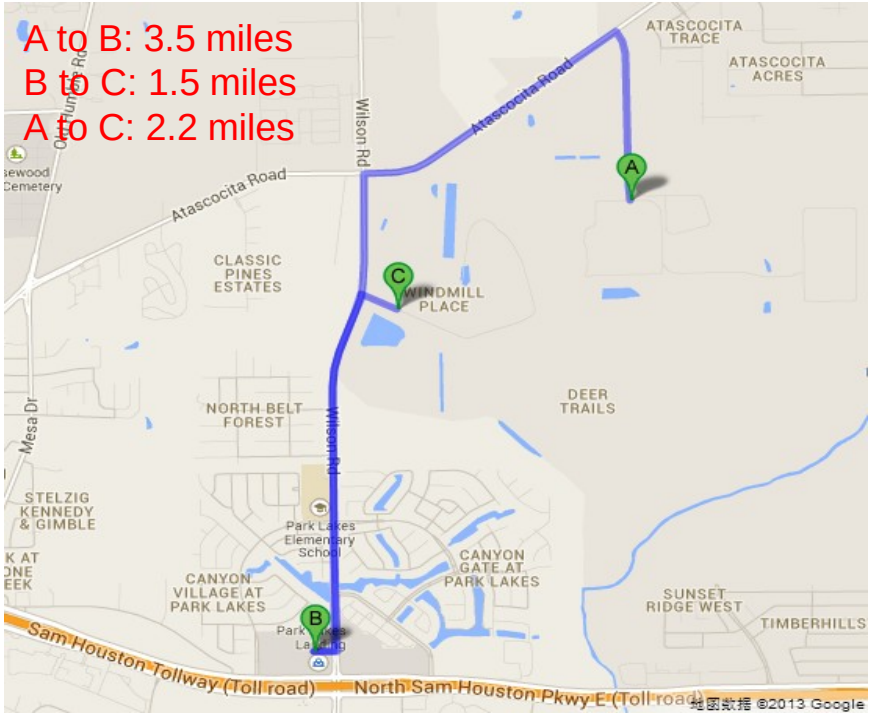

Atascocita Landfill, Humble, TX 77396
CH4 Perimeter Measurements

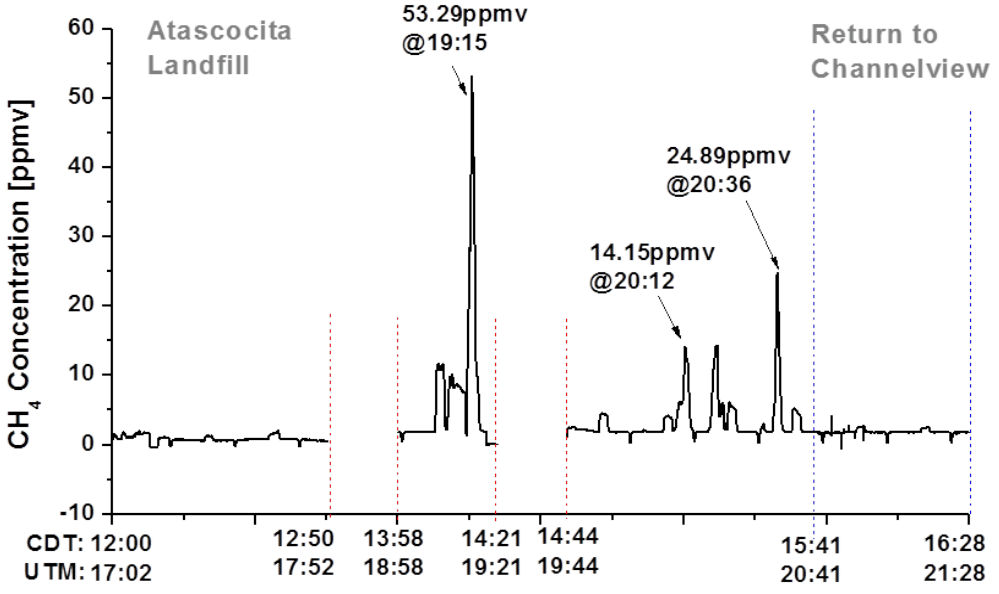

A: 29.9599º North, 95.2334º West
B: 29.9364º North, 95.2508º West
C: 29.9547º North, 95.2462º West (Landfill)

M. Jahjah et. al., Opt. Letters., 39, 957-960, 2014

Motivation of H_2O_2 Detection

- Oxidative capacity of atmosphere and balance of HO_x;
- Acid rain formation & In-cloud oxidation of S(IV) to S(VI);
- Active agent in decontamination and sterilization systems;
- H_2O_2 in breath is a biomarker of oxidative stress;
- H_2O_2 concentration levels in Houston have not been reported despite of atmospheric conditions, such as high humidity, high solar radiation levels, and the presence of the petrochemical industry.

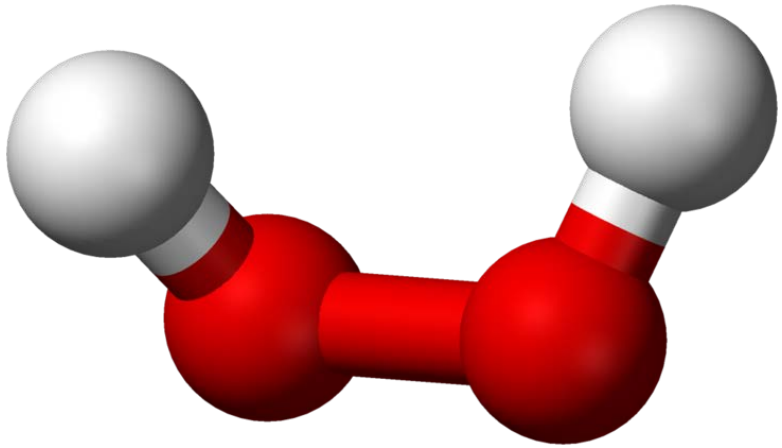

H_2O_2

RICE

QEPAS based Hydrogen Peroxide (H_2O_2) Sensor System

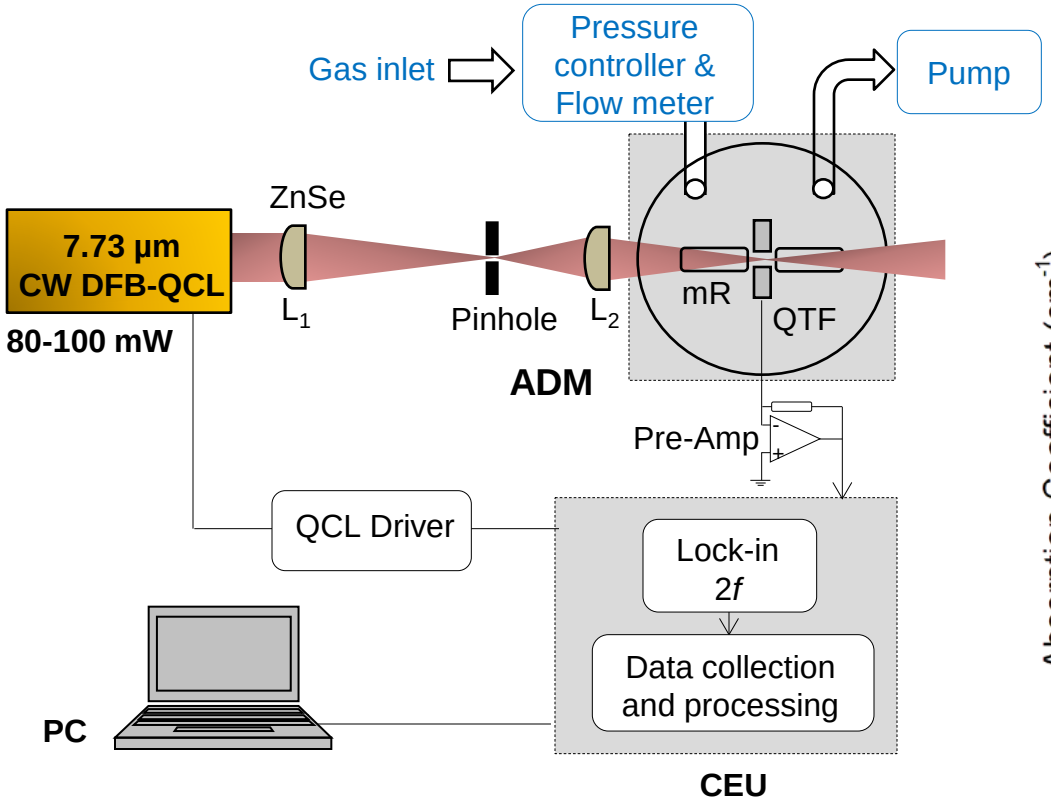

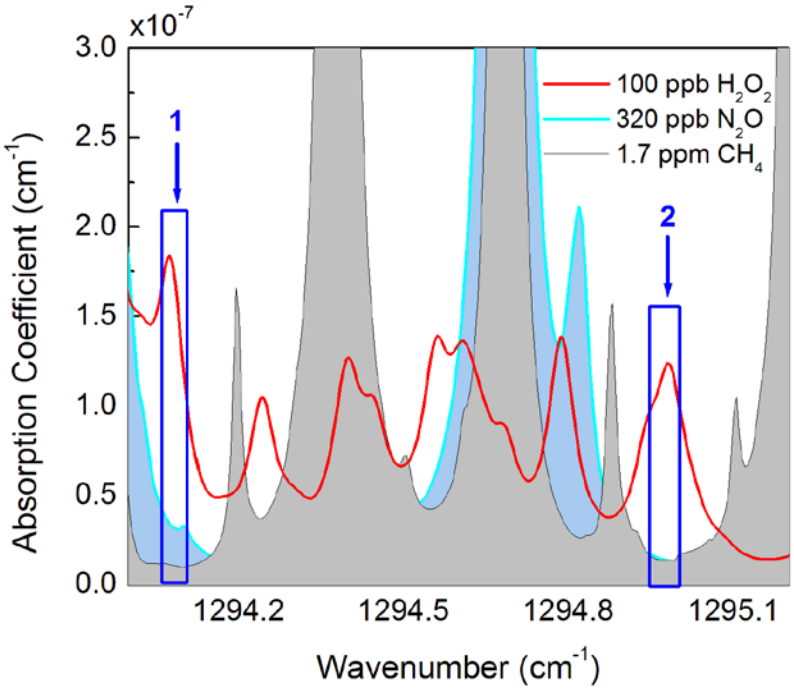

Schematic of QCL based QEPAS sensor:
ADM – acoustic detection module; CEU – control electronics unit; PC – personal computer.

Simulated spectra (HITRAN) of H_2O_2 at 296 K and 130 Torr, along with atmospheric interfering molecules of CH_4 and N_2O; two target wavelengths at 1294.1 and 1294.9 cm^{-1} are shown.

H_2O_2 Exposure limit is set at 1 ppmv by OSHA

RICE

W. Ren et al., Appl. Phys. Lett., 114, 041117, 2014

QEPAS Performance for Trace Gas Species (September 2014)

	Molecule (Host)	Frequency, cm^{-1}	Pressure, Torr	NNEA, $cm^{-1}W/Hz^{1/2}$	Power, mW	NEC (τ=1s), ppmv
VIS	O_3 (air)	35087.70	700	3.0×10^{-8}	0.8	1.27
	O_2 (N_2)	13099.30	158	4.74×10^{-7}	1228	13
NIR	C_2H_2 (N_2)*	6523.88	720	4.1×10^{-9}	57	0.03
	NH_3 (N_2)*	6528.76	575	3.1×10^{-9}	60	0.06
	C_2H_4 (N_2)*	6177.07	715	5.4×10^{-9}	15	1.7
	CH_4 (N_2+1.2% H_2O)*	6057.09	760	3.7×10^{-9}	16	0.24
	N_2H_4	6470.00	700	4.1×10^{-9}	16	1
	H_2S (N_2)*	6357.63	780	5.6×10^{-9}	45	5
	HCl (N_2 dry)	5739.26	760	5.2×10^{-8}	15	0.7
	CO_2 (N_2+1.5% H2O) *	4991.26	50	1.4×10^{-8}	4.4	18
Mid-IR	CH_2O (N_2:75% RH)*	2804.90	75	8.7×10^{-9}	7.2	0.12
	CO (N_2 +2.2% H_2O)	2176.28	100	1.4×10^{-7}	71	0.002
	CO (propylene)	2196.66	50	7.4×10^{-8}	6.5	0.14
	N_2O (air+5%SF_6)	2195.63	50	1.5×10^{-8}	19	0.007
	C_2H_5OH (N_2)**	1934.2	770	2.2×10^{-7}	10	90
	NO (N_2+H_2O)	1900.07	250	7.5×10^{-9}	100	0.003
	H_2O_2	1295.6	150	4.6×10^{-9}	100	12
	C_2HF_5 (N_2)***	1208.62	770	7.8×10^{-9}	6.6	0.009
	NH_3 (N_2)*	1046.39	110	1.6×10^{-8}	20	0.006
	SF_6	948.62	75	$2.7x10^{-10}$	18	$5x10^{-5}$ (50 ppt)

* - Improved microresonator
** - Improved microresonator and double optical pass through ADM
*** - With amplitude modulation and metal microresonator

NNEA – normalized noise equivalent absorption coefficient.
NEC – noise equivalent concentration for available laser power and τ=1s time constant, 18 dB/oct filter slope.

For comparison: conventional PAS 2.2 $\times10^{-9}$ $cm^{-1}W/\sqrt{Hz}$ for NH_3

Use of Canines in non-invasive & sensitive Cancer Detection

Bladder Cancer
Urine
Sensitivity 73%
Specificity 56-92%

Ovarian cancer
Carcinoma Tissue
Sensitivity 100%,Specificity 98%
Blood
Specificity 100%, Sensitivity 95%

Prostate Cancer
urine
Sensitivity 99%

Lung Cancer
Breath
Sensitivity 99%
Specificity 99%

Melanoma
Skin VOCs
Potential!

Breast Cancer
Breath
Sensitivity 88%
Specificity 98%

Colorectal cancer

	Sensitivity	Specificity
Breath	91%	99%
Stool	97%	99%

Breath 2014, Torun, Prof. T. Jezierski et al.,
Institute of Genetics and Animal Breeding, PAS

RICE

Advantages & Disadvantages of Canines in Cancer Detection

- **Advantages**
  - Non-invasive, safe and easy sample collecting
  - Relatively easy training and interpretation of dogs' indications
  - Odor samples can be tested several times
  - Extremely high detection sensitivity and specificity
  - Potential of VOCs are useful in search, rescue and emergency applications

- **Disadvantages**
  - To-date a "black-box technology"
  - It is a method based on earning a reward, which becomes unreliable after ~ 4 years
  - Variation of sensitivity and specificity
  - Re-training of dogs is not effective

Breath 2014, Torun, Prof. T. Jezierski et al.,
Institute of Genetics and Animal Breeding, PAS

RICE

Merits of QEPAS based Trace Gas Detection

- Very small sensing module and sample volume (a few mm^3 to ~$2cm^2$)
- Extremely low dissipative losses
- Optical detector is not required
- Wide dynamic range
- Frequency and spatial selectivity of acoustic signals
- Rugged transducer – quartz monocrystal; can operate in a wide range of pressures and temperatures
- Immune to environmental acoustic noise, sensitivity is limited by the fundamental thermal TF noise: $k_B T$ energy in the TF symmetric mode
- Absence of low-frequency noise: SNR scales as $\sqrt{t}$, up to t=3 hours as experimentally verified

QEPAS: some challenges

- Cost of Spectrophone assembly
- Sensitivity scales with laser power
- Effect of H_2O
- Responsivity depends on the speed of sound and molecular energy transfer processes
- Cross sensitivity issues

RICE

Future Directions and Outlook

- New target analytes: formaldehyde (CH_2O), ethylene (C_2H_4), ozone (O_3) and nitrate (NO_3
- Ultra-compact, low cost, robust sensors (e.g. CH_4, NO, CO…)
- QCL based ultra-portable atmospheric carbon isotope monitor for $^{12}CH_4$ & $^{13}CH_4$
- Monitoring of broadband absorbers: acetone (C_3H_6O): MDL of 1.5 ppm with a 7mW ICL & AM, or 20ppb with a 100mW QCL @ 8.23µm; benzene (C_6H_6)…
- Optical power build-up cavity designs (I-QEPAS)
- THz QEPAS based sensors
- Development of trace gas sensor networks

RICE

Potential Integration of a CW DFB- QCL and QEPAS Absorption Detection Module

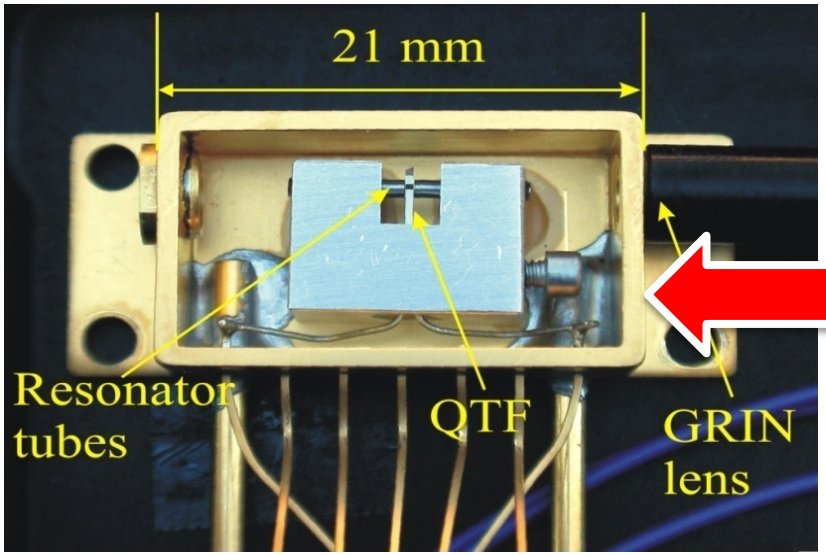

2012 QEPAS ADM

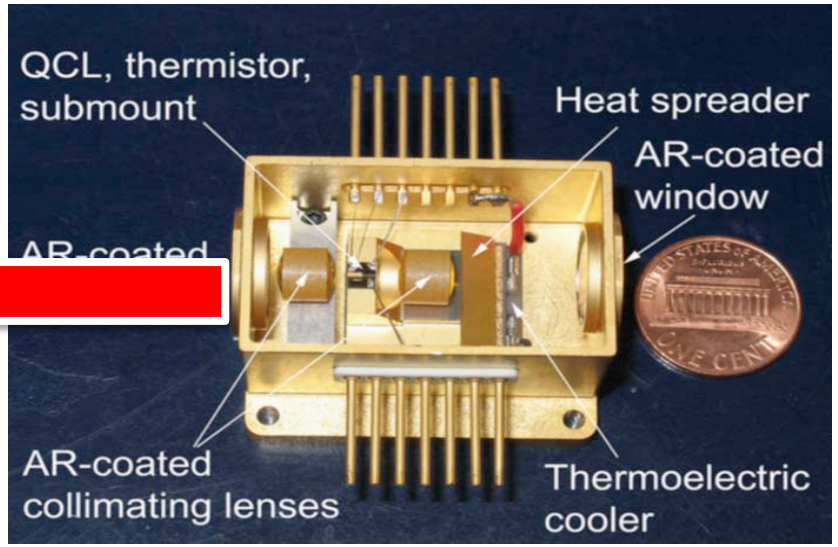

HHL package fiber coupled DFB-QCL

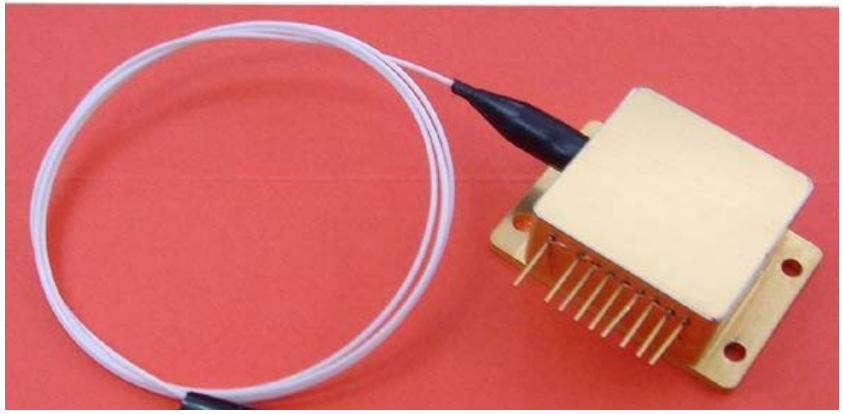

A. Lyakh, et al "1.6 W high wall plug efficiency, continuous-wave room temperature quantum cascade laser emitting at 4.6 μm", Appl. Phys. Lett. **92**, 111110 (2008)

Why is THz based Trace Gas Sensing useful ?

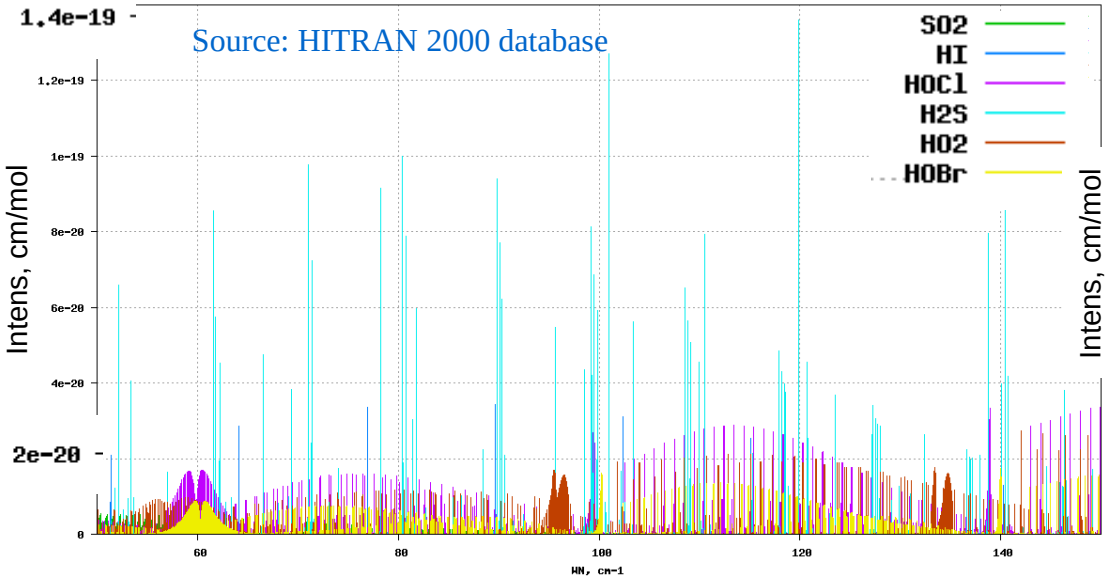

1.6 e-18

Several gas species such as HF, OH, HCN, HCl, HBr, NH_3, H_2O_2, H_2S, H_2O & explosives (in the vapor phase) show strong absorption bands in the THz spectral range.

Mainly rotational levels are involved in THz absorption processes and rotational-translational (R-T) relaxation rates are **up to three order of magnitude faster** with respect to vibrational-translational (V-T) in the mid-infrared

QEPAS signal strongly depends on the energy relaxation rates due to the possibility to **operate at low pressure**, & thereby taking advantages of the typically **very high QTF Q-factors.**

Why have QEPAS sensors not been developed in the THz spectral range so far?

Standard QTFs have a very small volume ($\sim 0.3 \times 0.3 \times 3\ mm^3$)

In QEPAS sensor systems , it is critical to avoid laser illumination of the QTF, since the radiation blocked by the QTF prongs results in an undesirable non-zero background as well as a shifting fringe-like interference pattern.

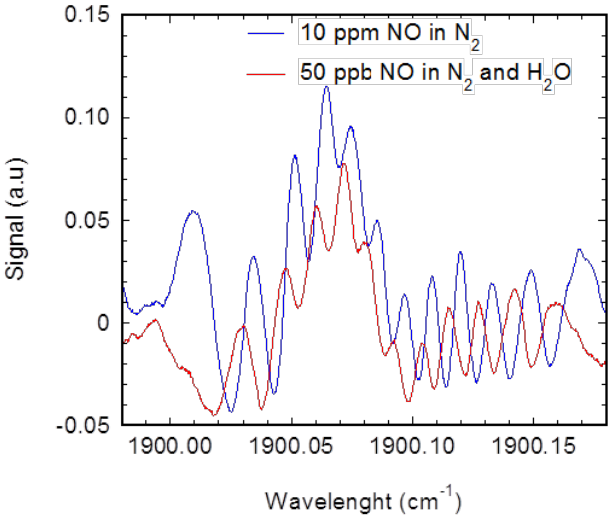

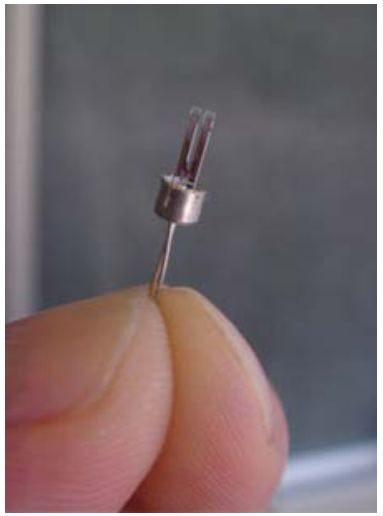

Standard QTF

The standard QTF prong separation of 330 µm is comparable with the THz wavelength which prevents the use of a QEPAS sensor architecture in the THz range unless we use large sized QTFs .

Custom fabricated QTFs scaled in Dimensions (~7 & 3 times larger) with respect to a standard QTF

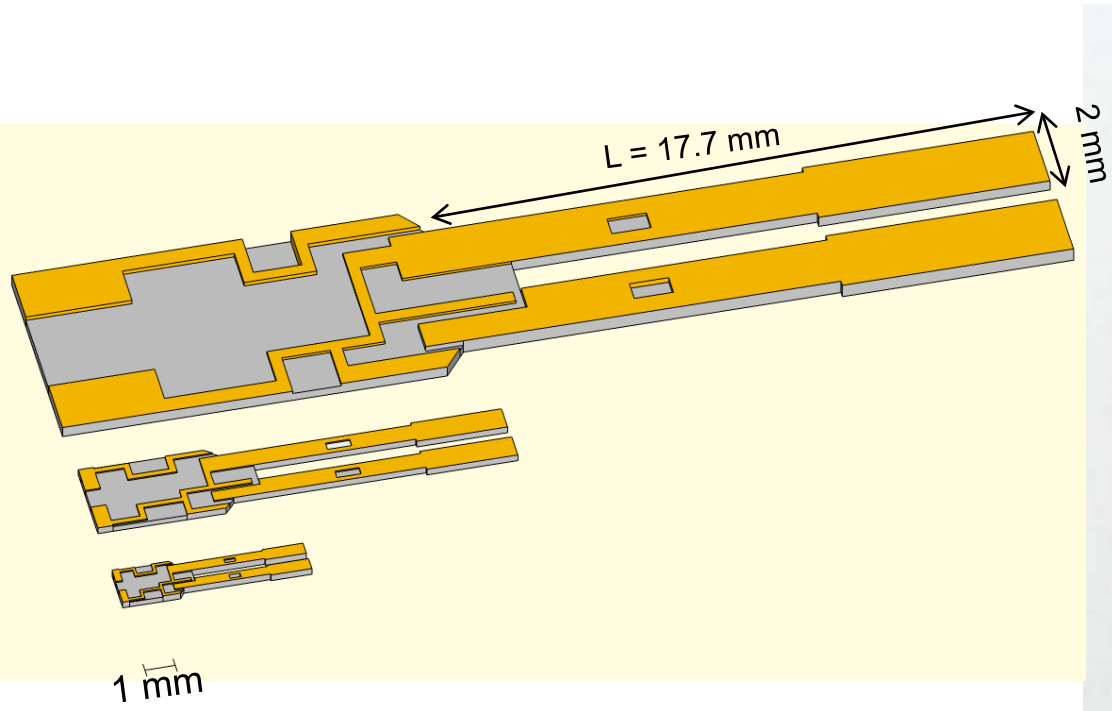

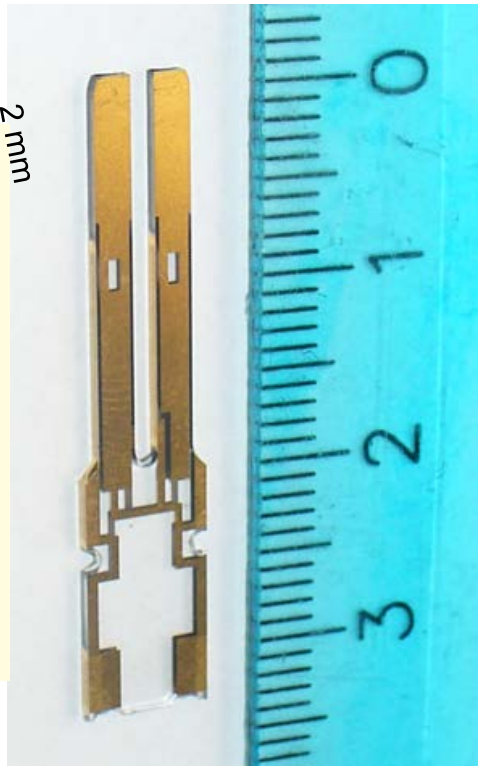

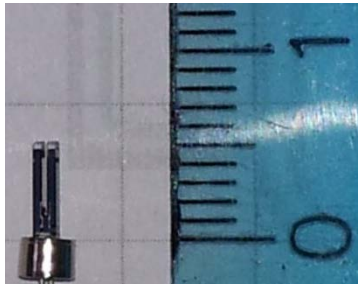

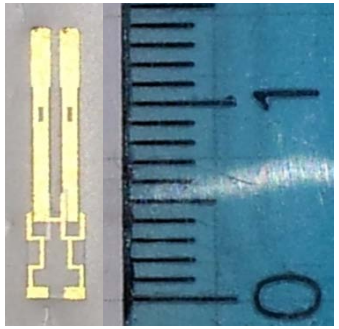

Standard photolithographic techniques were used to etch the custom QTF, starting from a z-cut quartz wafer. Chromium/gold contacts were deposited on both sides of the custom QTF.

Currently verification that the larger QTFs behave similar to a "standard" QTF in terms of vibrational modes and Q factor is in progress

THz QCL Sources via Nonlinear Optics

Use intra-cavity DFG in mid-IR QCLs

$$W(\omega_{THz}) \propto \left|\chi^{(2)}\right|^2 W(\omega_1) W(\omega_2) \times l_{eff}^2$$

THz QCL source based on intra-cavity DFG

- *Same fabrication/user operation as regular QCLs*
- *Room temperature operation*
- *Broadband THz tuning*

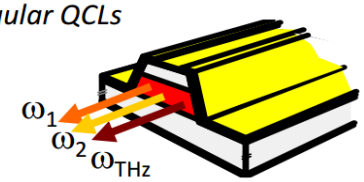

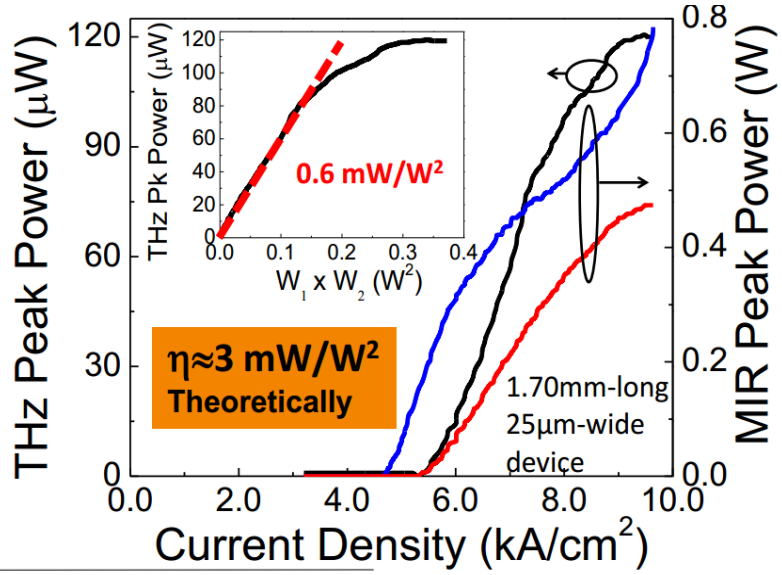

Vijayraghavan *et al., Nature Comm.* ***4,*** *2021* (2013)

2.3-mm-long, 22-μm-wide device @ room temperature

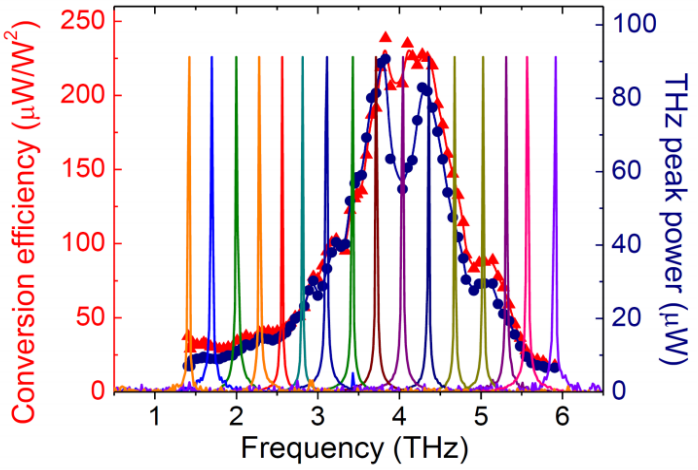

IQCLSW 2014, Policore, Italy: M.A. Belkin et al, UT Austin, USA

Vijayraghavan *et al., Nature Comm.* ***4,*** *2021* (2013); Jiang *et al., J. Opt.* **16,**094002 (2014)

Monolithic tuners: 0.58 THz of tuning – Jung *et. al., Nature Comm.* ***5,*** *4267* (2014)

THz QEPAS Sensor System for Methanol (CH_3OH) Detection

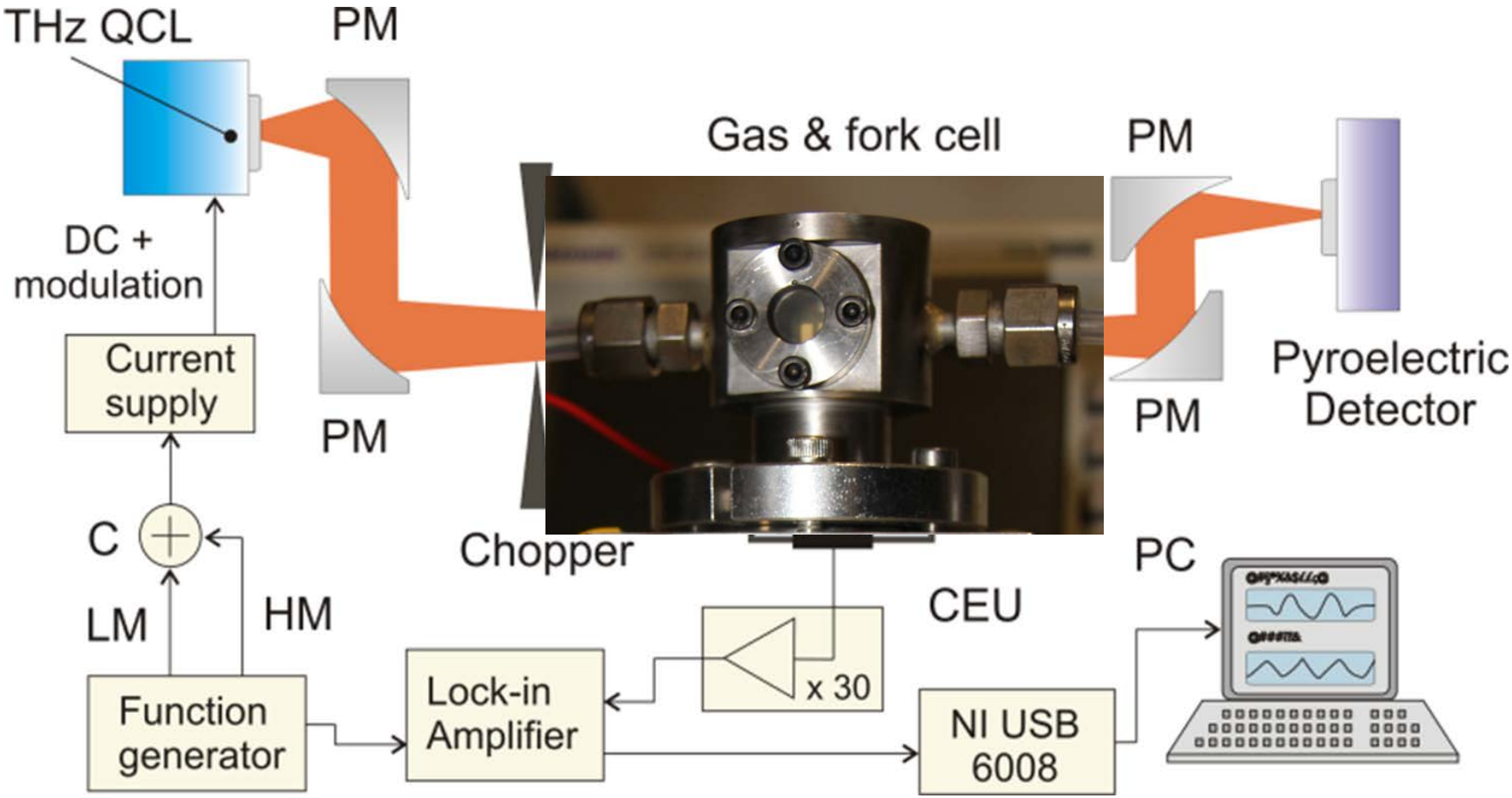

Legend

PM – parabolic mirror
QTF – quartz tuning fork
C – power combiner
LM - low-frequency modulation (ramp)
HM -high-frequency modulation
CEU- control electronics unit

THz QEPAS Performance in Locked Mode and Long-term Stability

Stepwise methanol concentration measurements

- *Lock-in* $\tau = 100$ *ms*

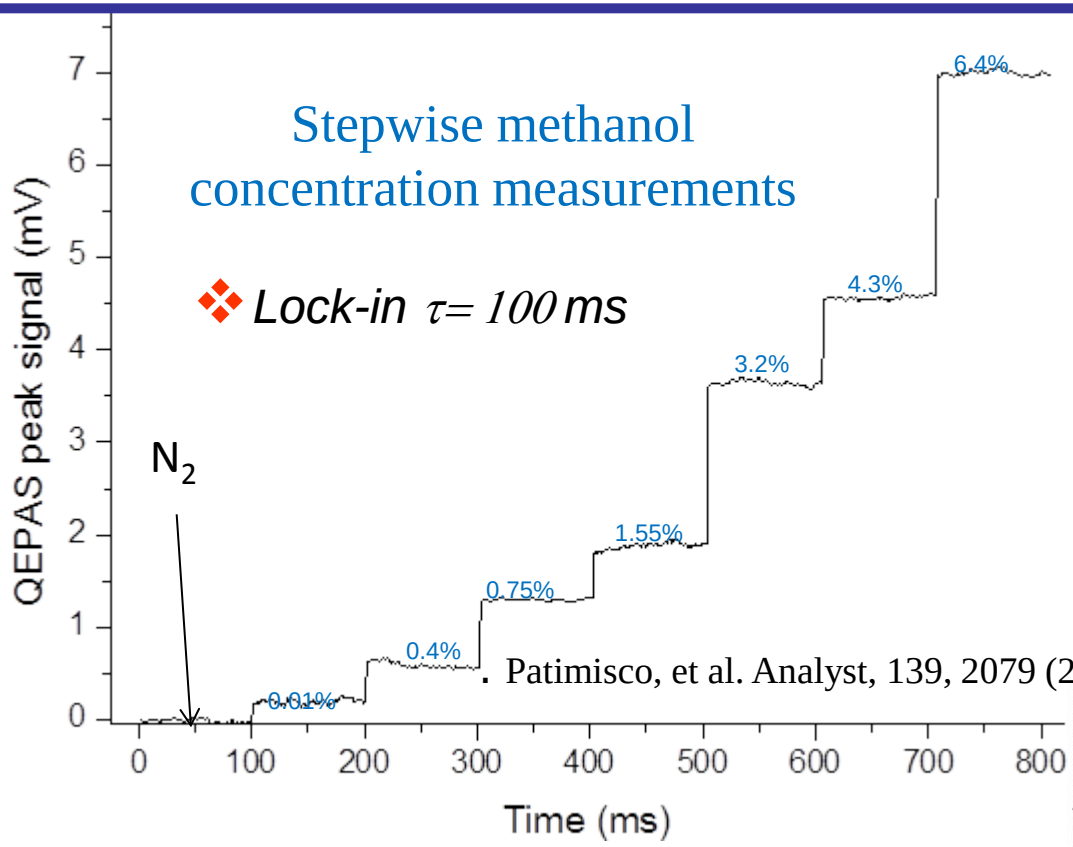

. Patimisco, et al. Analyst, 139, 2079 (2014)

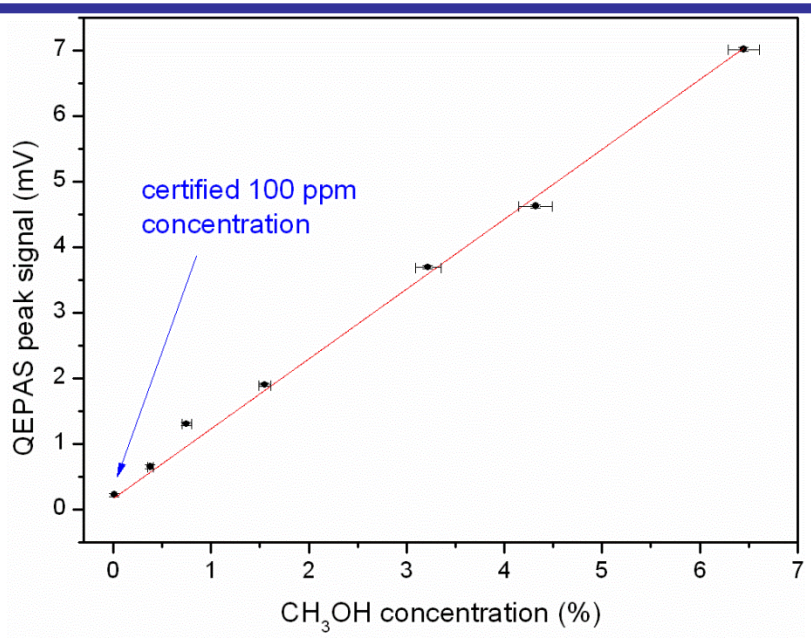

NEC= 7 ppm (@ a laser power of 40 µW & a 4sec lock-in constant)

Absorption coefficient normalized to detection bandwidth and optical power:

NNEA = 2.0 x10^{-10} cm^{-1}W(Hz)$^{-1/2}$

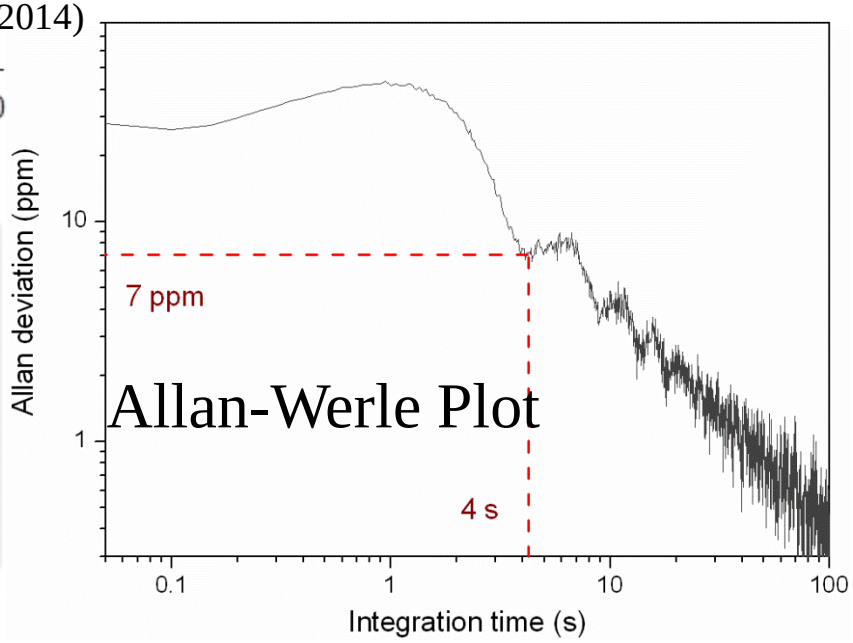

Proposed Intracavity-QEPAS (I-QEPAS) Sensor System

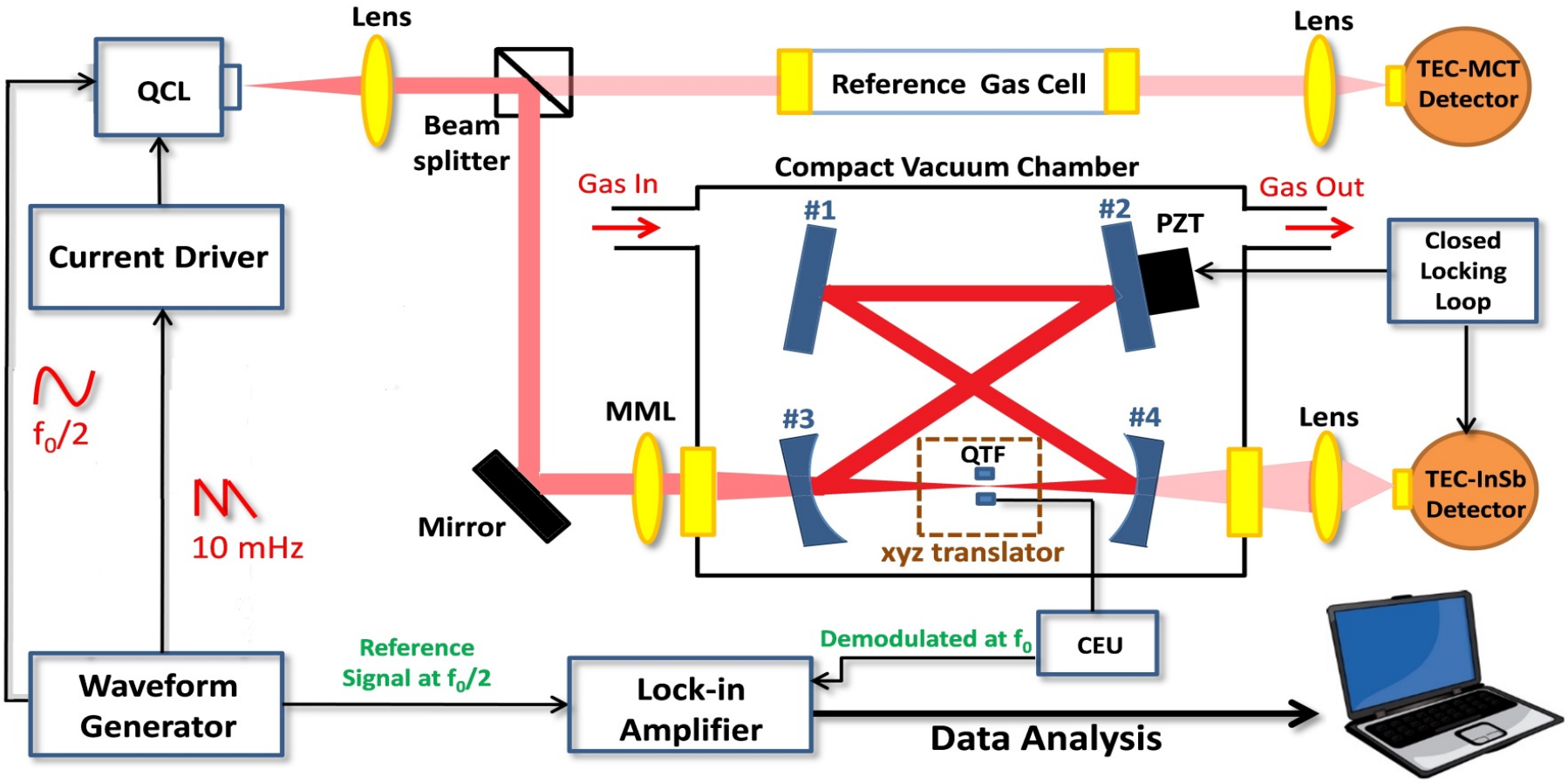

Optical power build up cavity can provide:

- **RT CW DFB QCL, λ=4.33 microns**
- **Low noise current driver → narrow QC laser linewidth ~1 MHz**
- **Bow-tie cavity →4 high reflectivity mirrors, R=99.9%**
- **Electronic Control Loop + PZT driver lock of cavity resonant frequency to QCL frequency**

P. Patimisco, G. Scamarcio, F.K. Tittel & V. Spagnolo, "Quartz-enhanced photoacoustic spectroscopy: a review", Sensors, 14, 6165-6206 (2014)

Comparison of I-QEPAS with Other Trace Gas Sensing Techniques

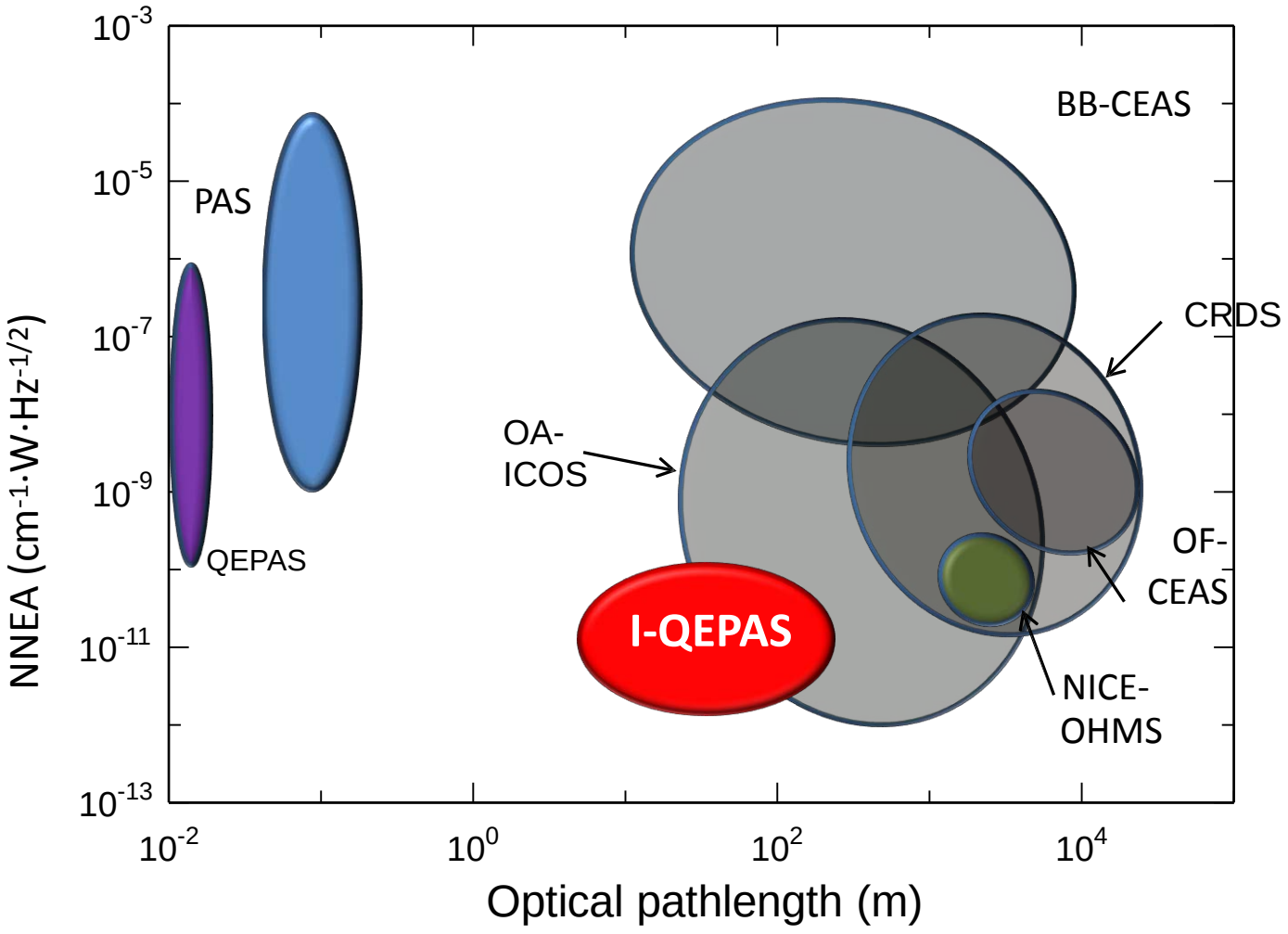

P. Patimisco, G. Scamarcio, F.K. Tittel & V. Spagnolo, "Quartz-enhanced photoacoustic spectroscopy: a review", Sensors, 14, 6165-6206 (2014)

Cylindrical Multi-pass Trace Gas Absorption Cell

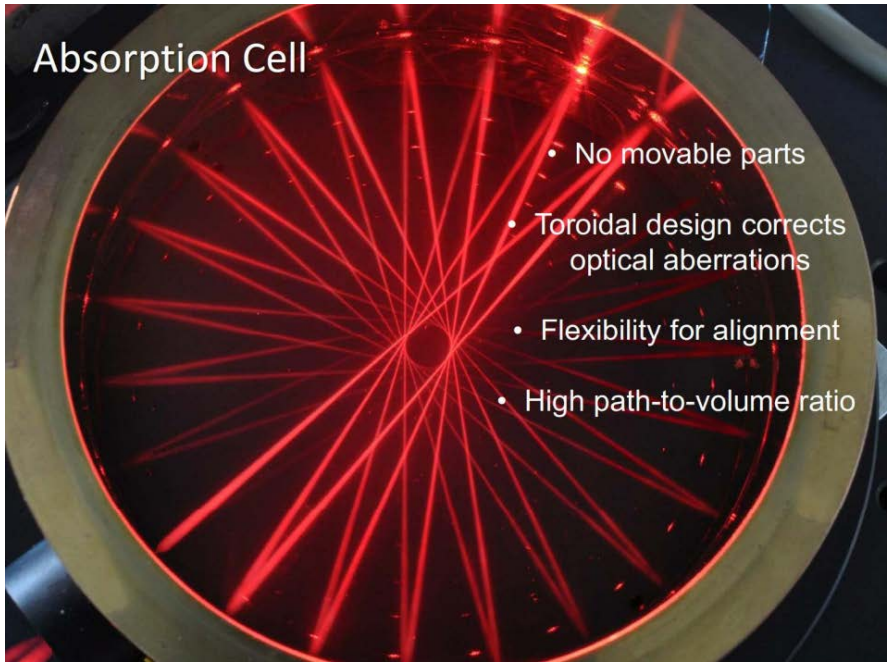

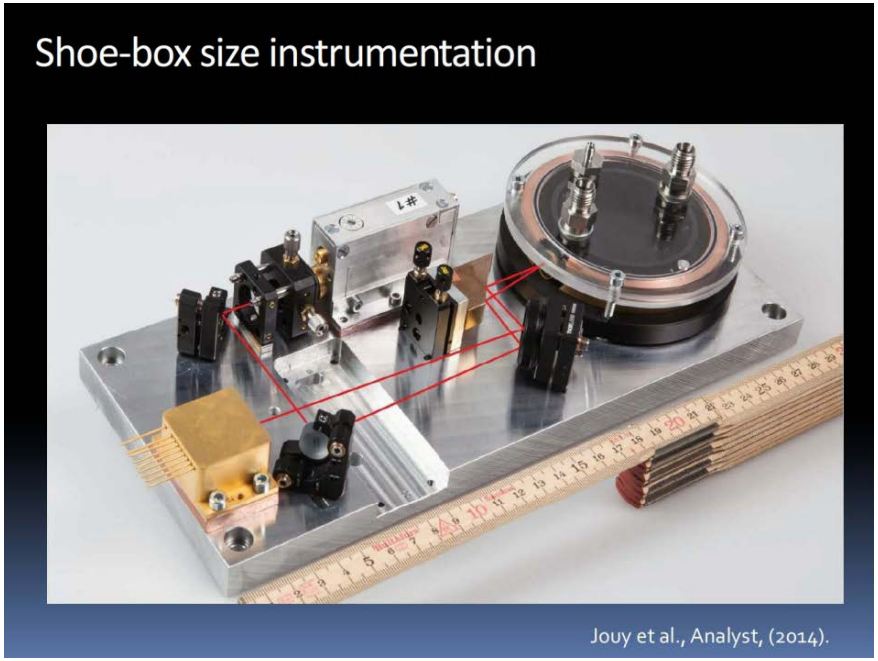

L. Emmenegger et al, IQCLSW 2014, Policore, Italy

NO_2 Sensitivity Test at Jungfraujoch (3850m asl), Switzerland

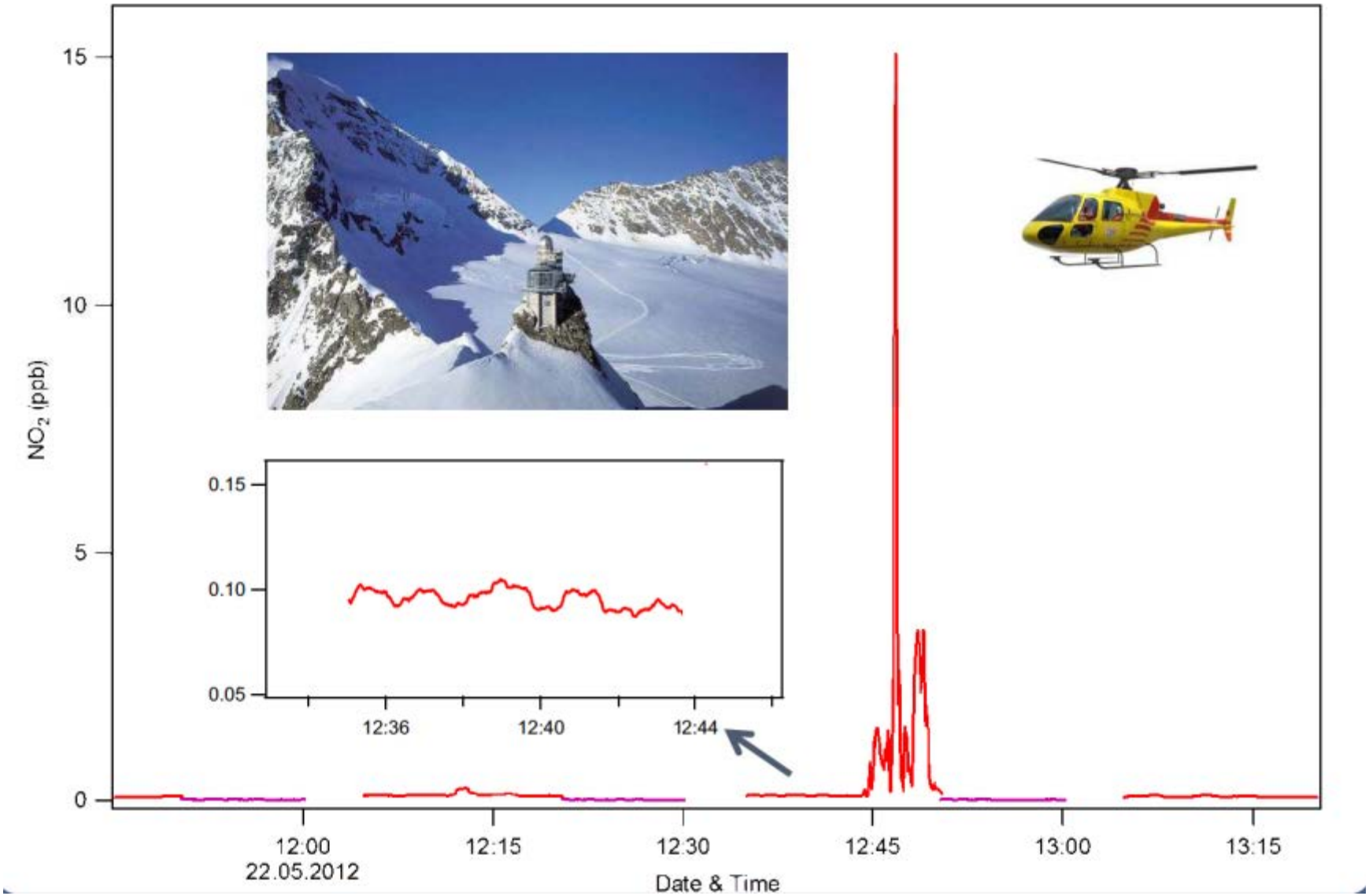

L. Emmenegger et al, IQCLSW 2014, Policore, Italy

Isotopic Ratio Measurements of $\delta^{18}O$ (‰) & $\delta^{13}C$ (‰) performed at the Jungfraujoch (3850m asl), Switzerland

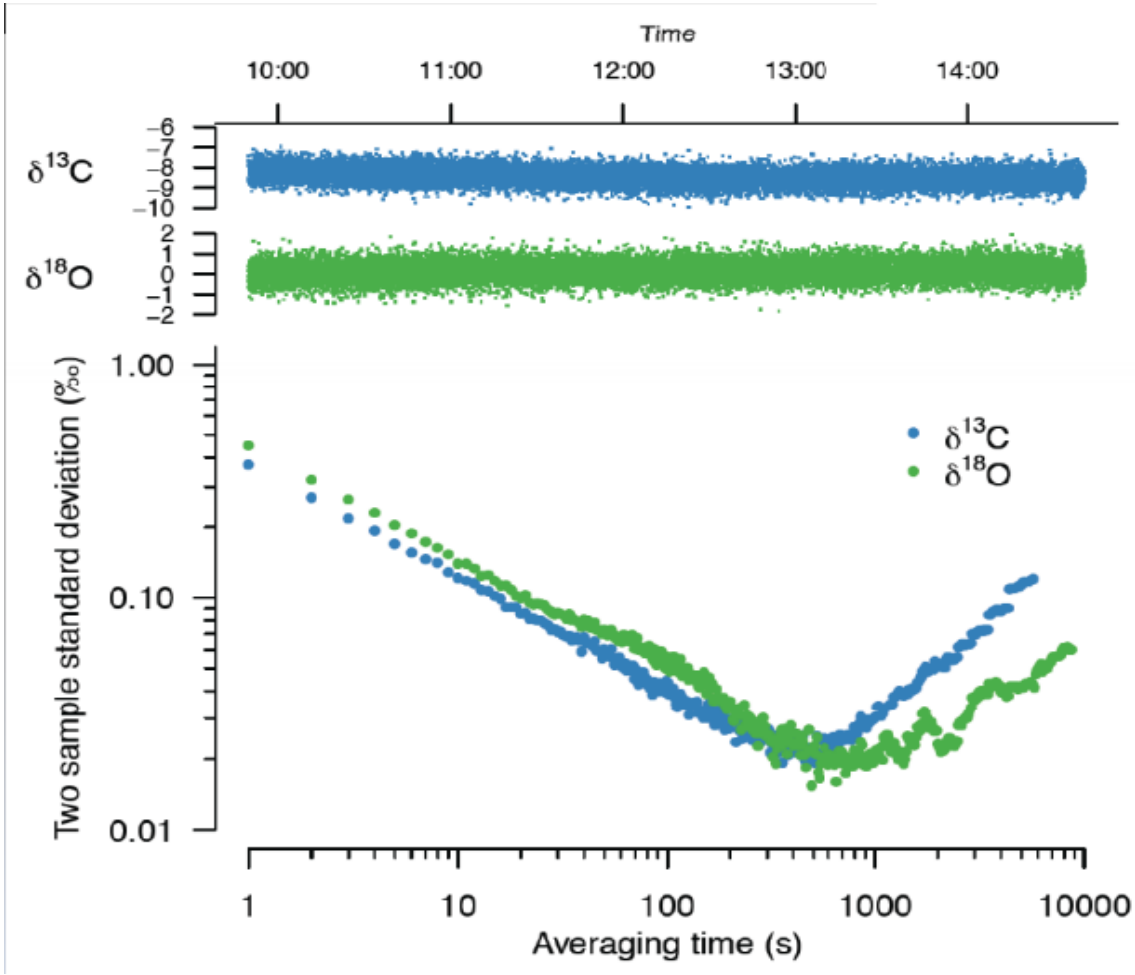

Precision (1σ)	
1 s:	0.5 ‰
60 s	< 0.07 ‰
600 s	< 0.03 ‰

Year	$1\sigma_{min}$
2006	0.16 ‰
2009	0.046 ‰
2012	0.025 ‰

Allan-Werle variance plot

L. Emmenegger et al, IQCLSW 2014, Policore, Italy

Summary and Conclusions

- Development of robust, compact, sensitive, selective mid-infrared trace gas sensor technology based on room temperature, continuous wave DFB laser diodes and high performance QCLs for environmental monitoring and medical diagnostics.
- Interband cascade and quantum cascade lasers were used in TDLAS, PAS and QEPAS based sensor platforms
- Eight target trace gas species were detected with a 1 sec sampling time:
  - C_2H_6: ~3.36 µm, detection sensitivity of 740 pptv using TDLAS
  - NH_3: ~10.4 µm, detection sensitivity of ~1 ppbv (200 sec averaging time)
  - NO: ~5.26 µm, detection limit of 3 ppbv
  - CO: ~4.61 µm, minimum detection limit of 2 ppbv
  - SO_2: ~7.24 µm, detection limit of 100 ppbv
  - CH_4 and N_2O: ~7.28 µm, detection limits of 13 and 6 ppbv, respectively
  - H_2O_2: ~7.73 µm, detection limit of 75 ppb

  :
- New target analytes: CH_2O and C_2H_6O

RICE